β-lactam Antibiotics Stimulate the Pathogenicity of Methicillin-resistant *Staphylococcus aureus* Via SarA-controlled Tandem Lipoprotein Expression

Weilong Shang[1¶], Yifan Rao[2¶], Ying Zheng[1¶], Yi Yang[1], Qiwen Hu[1], Zhen Hu[1], Jizhen Yuan[1], Huagang Peng[1], Kun Xiong[1], Li Tan[1], Shu Li[1], Junmin Zhu[1], Ming Li[1], Xiaomei Hu[1], Xuhu Mao[2,3*], Xiancai Rao[1*]

[1] Department of Microbiology, College of Basic Medical Sciences, Army Medical University (Third Military Medical University), Chongqing, 400038, China,

[2] Institute of Modern Biopharmaceuticals, School of Life Sciences, Southwest University, Chongqing, 400715, China,

[3] Department of Clinical Microbiology and Immunology, College of Medical Laboratory Science, Army Medical University (Third Military Medical University), Chongqing, 400038, China.

¶These authors contributed equally to this work.

* Corresponding author

E-mail: X. Rao: raoxiancai@126.com, or X. Mao: mxh95xy@tom.com.

Running title: β-lactams stimulate MRSA pathogenicity

Abstract

Methicillin-resistant *Staphylococcus aureus* (MRSA) is a leading cause of nosocomial infections worldwide. MRSA resists nearly all β-lactam antibiotics that have a bactericidal activity and a signal inducer effect. However, studies have yet to clarify whether the inducer effect of empirically used β-lactams stimulates MRSA pathogenicity in vivo. Here, we showed that a new cluster of tandem lipoprotein genes (*tlpps*) was upregulated in MRSA in response to the subinhibitory concentrations of β-lactam induction. The increased Tlpps significantly altered immune responses by macrophages with high IL-6 and TNFα levels. The deletion of the *tlpps* mutant (N315Δ*tlpps*) significantly decreased the proinflammatory cytokine levels in vitro and in vivo. The bacterial loads of N315Δ*tlpps* in the mouse kidney were also reduced compared with those of the wild type N315. The β-lactam-treated MRSA exacerbated cutaneous infections with increased lesion size, extended illness, and flake-like abscess-formation compared with those of the nontreatment. The β-lactam antibiotics that promoted the MRSA pathogenicity were SarA dependent, and the increasing expression of *tlpps* after β-lactam treatment was directly controlled by the global regulator SarA. Overall, our findings suggested that β-lactams should be used carefully because it might lead to a worse outcome of MRSA infection than inaction in the treatment.

Key words: Methicillin-resistant *Staphylococcus aureus*, β-lactam antibiotics, tandem lipoproteins, SarA, pathogenicity

Author summary

β-lactams are widely used in practice to treat infectious diseases, however, β-lactams worsening the outcome of a certain disease is poorly understood. In this study, we have identified a new cluster of tandem lipoprotein genes (*tlpps*) that is upregulated in the major clinically prevalent MRSA clones in response to the subinhibitory concentrations of β-lactams induction. The major highlight in this work is that

β-lactams induce SarA expression, and then SarA directly binds to the *tlpp* cluster promoter region and upregulates the *tlpp* expression in MRSA. Moreover, the β-lactam stimulated Tlpps are important virulence factors that enhance MRSA pathogenicity. The deletion of the *tlpps* mutant significantly decreases the proinflammatory cytokine levels in vitro and in vivo. The β-lactam induced Tlpps enhance the host inflammatory responses by triggering the expression of IL-6 and TNFα, thereby promoting bacterial colonization and abscess formation. These data elucidate that β-lactams can worsen the outcome of MRSA infection through the induction of *tlpps* that are controlled by the global regulator SarA.

Introduction

Infectious diseases caused by bacteria are common and adversely affect human health worldwide. The discovery of antibiotics for antibacterial application was a remarkable achievement in the 20th century. In the therapeutic use of antibiotics in humans and animals, bacteria encounter wide gradients of antibiotic concentrations in host bodies [1]. Antibiotics can serve as signal inducers, in addition to their clinically important antibacterial activity, and influence the physiological characteristics of bacteria and trigger various cellular responses in bacterial species. Low levels of antibiotics can induce extracellular DNA release, virulence factor production, and biofilm formation [2,3], resulting in a worse outcome of bacterial infections. Therefore, the mechanisms underlying the stimulation of pathogenicity in a bacterial population at subinhibitory antibiotic concentrations should be understood.

Methicillin-resistant *Staphylococcus aureus* (MRSA) is a leading pathogen with notable pathogenic effects. MRSA causes a wide range of diseases, including acute skin and soft tissue infections, chronic and persistent endocarditis, osteomyelitis, and pneumonia [4,5]. MRSA infections cause greater morbidity and mortality than methicillin-susceptible *S. aureus* (MSSA) infections do [6,7]. However, the underlying mechanisms of these effects remain unclear. Several studies have suggested that as-yet-unidentified virulence factors or inappropriate treatments

contribute to the poor outcome of MRSA infections [6,8,9]. It has been reported that between 30% and 80% of individuals infected with MRSA are inappropriately treated often with β-lactam antibiotics because of the failure to recognize MRSA infection initially [10,11]. Accumulated data have demonstrated that the subinhibitory concentrations of β-lactam antibiotics can promote *S. aureus* pathogenicity by increasing the expression of alpha-toxin [12], Panton–Valentine leukocidin (PVL) [2], enterotoxins [13], or staphylococcal protein A (SPA) in vitro [14]. Nevertheless, the contribution of the certain altered virulence factor to the MRSA pathogenesis in vivo has yet determined, and the molecular mechanisms underlying β-lactams modulating MRSA pathogenesis remain largely unknown.

Lipoproteins (Lpps) are an abundant family of proteins anchored in the bacterial membrane, and they account for at least 2% of a bacterial proteome [15,16]. *S. aureus* encodes 55–70 putative Lpps, and approximately 50% of these Lpps are annotated as chaperones or as transporters for amino acids, peptides, iron, and zinc [17]. Many of the proposed Lpps (more than 30%) in *S. aureus* are conserved hypothetical proteins of unknown functions [16]. Most virulent MRSA strains, such as USA300, carry a conserved genomic island termed νSaα (nonphage and nonstaphylococcal cassette chromosome genomic island) that encodes numerous homologous *lpps* arranged in tandem, which is referred to as "tandem lipoproteins" (*tlpps*) or "lipoprotein-like" (*lpl*) [15,18]. This *tlpp* cluster likely represents the paralogous genes that have diverged after a duplication event in *S. aureus* [17]. MRSA USA300 belonging to the clonal complex CC8 carries 15 (22%) hypothetical Tlpps. Of these Tlpps, 9 are specific to the νSaα genomic island [15]. By comparison, N315 belonging to the clonal complex CC5 carries 12 (21%) hypothetical Tlpps. Of these Tlpps, 9 Lpl proteins are specific to the νSaα genomic island (S1 Table).

Some staphylococcal Lpps can trigger host cell invasion, increase bacterial pathogenicity, and contribute to the epidemic of CC8 and CC5 strains [19,20]. However, the exact roles of the Tlpp proteins are unclear. Whether these Tlpp proteins can be induced by the subinhibitory concentrations of antibiotics and contribute to the pathogenesis of MRSA have yet to be determined. In this study, we

118 demonstrated that a new *tlpp* cluster of MRSA was upregulated in response to the
119 subinhibitory concentrations of β-lactam induction. The increased Tlpps in MRSA
120 significantly altered immune responses by increasing the IL-6 and TNFα levels of the
121 macrophages. Null Tlpp MRSA mutant infection decreased the IL-6 and TNFα levels
122 in serum and the bacterial burdens in kidney of a mouse model. β-lactam-treated
123 MRSA N315 exhibited an increased pathogenicity with severe cutaneous infection
124 and abscess formation. Moreover, the β-lactam antibiotics that promoted
125 pathogenicity in MRSA were SarA dependent, and the increasing Tlpp expression
126 after β-lactam treatment was directly controlled by the global regulator SarA.
127

128 ## Results

129 **β-lactam antibiotics stimulated tandem lipoprotein expression in MRSA.**

130 It is reported that the subinhibitory concentrations of β-lactam antibiotics can induce
131 the production of some *S. aureus* toxins, such as alpha-toxin [12], PVL [2], and
132 enterotoxins [13], or immune evasion molecules, such as SPA [14]. Here, *S. aureus*
133 N315, which is a globally prevalent sequence type 5 (ST5) MRSA strain [21], was
134 tested for its antibiotic response to identify new factors contributing to MRSA
135 pathogenesis in antibiotic induction. The minimal inhibitory concentrations (MICs) of
136 β-lactam antibiotics, including oxacillin (OXA), methicillin (MET), cefoxitin (FOX),
137 imipenem (IMI), meropenem (MER), chloramphenicol (CHL), vancomycin (VAN),
138 kanamycin (KAN), and erythromycin (ERY) against N315 were determined (S2
139 Table). The sodium dodecyl sulfate–polyacrylamide gel electrophoresis (SDS-PAGE)
140 revealed that a protein band (approximately 30 kDa) was upregulated in the
141 subinhibitory concentrations of β-lactam-treated bacteria compared with the
142 nontreatment control (Fig 1A). By contrast, CHL, VAN, KAN, and ERY did not have
143 induction effects on this protein band. Further observations indicated that the
144 subinhibitory concentrations of OXA exerted a broad-spectrum induction effect on
145 other major clinically prevalent MRSA clones, including ST88, ST239, ST59, ST1,
146 and ST398, which displayed the same upregulated protein band as that in the

147 OXA-treated MRSA compared with the nontreatment one (Fig 1B).

148 The protein band was excised from the SDS-PAGE gel and analyzed through
149 liquid chromatography tandem mass spectrometry (LC-MS/MS) to characterize the
150 β-lactam-induced proteins in the MRSA strains. The detected peptides matched with
151 68 proteins in the N315 proteome (S3 Table). Most known metabolic enzymes were
152 excluded, and three putative Tlpps, namely, Tlpp3 (SA2273), Tlpp2 (SA2274), and
153 Tlpp1(SA2275), encoded by a consecutive gene cluster were selected on the basis of
154 theoretical molecular weights for the analysis (Fig 2A and S1 Table). SA2273,
155 SA2274, and SA2275 were annotated as hypothetical proteins in the N315 genome
156 (GenBank accession no. BA000018.3). A typical Lpp precursor contained a signal
157 peptide at the N-terminal and a characteristic conserved three-amino acid lipobox in
158 front of the invariable cysteine [(LVI) (ASTG) (GA)↓**C**] [16,17]. Both Tlpp1 and
159 Tlpp3 possessed signal peptides and "lipobox" sequences, whereas Tlpp2 comprised a
160 transmembrane helix domain at the N-terminal (S1A Fig). These proteins were
161 annotated as Tlpps belonging to a domain of unknown function (DUF) 576 protein
162 family on the Pfam database [22]. Considering that Tlpps account for more than
163 62.6% of amino acid identity (S1B Fig), we prepared recombinant Tlpp1 proteins (Fig
164 1C) and the corresponding antibodies, and verified the authority of the
165 β-lactam-stimulated proteins through Western blot analysis (Fig 1D). Although
166 several MRSA clones, such as ST8 and ST239, contained only two of the three *tlpps*
167 in their genomes, the *tlpp* cluster was widely distributed among the major prevalent
168 MRSA clones (S4 Table). This observation was consistent with the finding that
169 several major MRSA clonal strains upregulated Tlpps in response to the subinhibitory
170 concentrations of β-lactam treatment (Fig 1B).
171
172 **_tlpp1_, _tlpp2_, and _tlpp3_ were co-transcribed, and their expression was induced by**
173 **β-lactam antibiotics in a dose- and time-dependent manner**
174 Reverse-transcription polymerase chain reaction (RT-PCR) was performed using
175 RNA extracted from MRSA N315 by specific primers to test whether *tlpp1*, *tlpp2*,
176 and *tlpp3* were co-transcribed (Fig 2A and S5 Table). The comparison of the RT-PCR

177 results with the template of the genomic DNA or RNA only revealed that *tlpp1*, *tlpp2*,
178 and *tlpp3* were co-transcribed from the *tlpp1* promoter (Fig 2B). We further examined
179 the influence of β-lactams on *tlpp* expression. Reverse-transcription quantitative PCR
180 (RT-qPCR) showed that the mRNA levels of *tlpp1*, *tlpp2*, and *tlpp3* were upregulated
181 in N315 after treatment with the subinhibitory concentrations of OXA (Fig 2C).
182 Western blot analysis demonstrated that the protein levels of Tlpps in both N315 total
183 cell lysates (Fig 2D and 2E) and the culture supernatant (Fig 2F and 2G) increased in
184 a dose-dependent manner after OXA treatment was administered. Tlpp expression
185 was also upregulated by N315 in a dose-dependent manner after MET treatment was
186 given (S2 Fig). Furthermore, the Tlpp expression by N315 increased in a
187 time-dependent manner after OXA treatment was administered (Fig 2H and 2I). These
188 results verified that MRSA Tlpps could be released from the bacteria and secreted to
189 the culture, and their production was influenced by the subinhibitory concentrations of
190 β-lactam antibiotics.
191
192 **β-lactam-induced Tlpps triggered proinflammatory cytokine production by**
193 **macrophages**
194 In Gram-negative bacteria, the cell wall-associated lipopolysaccharides are the main
195 molecules involved in activating the innate immune system of hosts via TLR4
196 interaction [23], while in Gram-positive bacteria, the releasable Lpps may be the main
197 factor that exert a similar function by triggering the TLR2-MyD88-NF-κB signaling
198 pathway, thereby inducing proinflammatory cytokines [17,19]. To determine whether
199 the β-lactam-induced MRSA Tlpps involved in the innate immune activation, we
200 cultured mouse RAW264.7 macrophages in media containing 5% culture supernatant
201 of N315 post-treated with different concentrations of OXA for 6 h. We then
202 determined the levels of proinflammatory cytokines, such as IL-6 and TNFα, in the
203 cell-cultured media (DMEN). The results revealed that IL-6 and TNFα levels were
204 gradually increased by macrophages stimulated by the culture supernatant of N315
205 treated with OXA in a dose-dependent manner (Fig 3A and 3B). Then, we wondered
206 whether the MRSA Tlpps promoted the cytokine expression in macrophages, a *tlpps*

deletion mutant (N315Δ*tlpp*s) with a pYT3-Δ*tlpps* plasmid and a *tlpps*-overexpressing strain (N315Δ*tlpp*s/pLI-*tlpps*) with a pLI-*tlpps* plasmid (Fig 3C and S3 Fig) were constructed for macrophage infection. Results showed that the production of IL-6 and TNFα in macrophages significantly decreased after treated with N315Δ*tlpp*s at a multiplicity of infection (MOI) of 30 compared with those of the wild-type N315 administered. By contrast, higher levels of IL-6 and TNFα were detected in macrophages treated with N315Δ*tlpp*s/pLI-*tlpps* but not with N315Δ*tlpp*s, which carried an empty pLI50 vector (Fig 3D and 3E). Similar results were observed when the bacterial culture supernatant was used (Fig 3G and 3H) because of the loss of Tlpp expression in the supernatant of N315Δ*tlpp*s (Fig 3F), indicating that the increased levels of IL-6 and TNFα by macrophages depended on the expression of N315 Tlpps that responded to β-lactams in a dose-dependent manner. However, the recombinant Tlpp1 purified from *Escherichia coli* (Fig 1C) exhibited no effect on the levels of IL-6 and TNFα by macrophages (S4 Fig), suggesting that a correctly triacylated Tlpp or a long-chain N-acylated Lpp was needed for the recognition by TLR2–TLR1 receptors to trigger immune response by macrophages [24].

Tlpps contributed to the virulence of MRSA

Consistent with the observed immune response by macrophages, the levels of IL-6 and TNFα in mice 6 h post-challenge with 1×10^7 N315Δ*tlpps* cells by tail vein injection were significantly lower than those of N315 was administered (Fig 4A and 4B). The complementary overexpression of *tlpps* (N315*Δtlpps*/pLI-*tlpps*) strain stimulated even higher levels of IL-6 and TNFα in mice, but not of the empty pLI50 plasmid-carrying strain (N315*Δtlpps*/pLI50). We also investigated whether the *tlpp* cluster of MRSA was associated with the bacterial burden in a mouse model. The mice were infected intravenously with pGFP plasmid-transformed N315 and N315Δ*tlpps* for 5 days (S6 Table), and bacterial colonization was tracked through an animal imaging system. The fluorescence intensity of the GFP in the murine organs (i.e., heart, lung, liver, spleen, and kidney) was measured, and the results indicated that the radiant efficiency in the kidneys of the mice injected with N315 was

significantly higher than those infected with N315Δ*tlpps* (Fig 4C and 4D). Consistent with the radiant efficiency, the bacterial loads in the kidneys of the N315-infected mice were also significantly higher than that of the N315Δ*tlpps*-infected ones (Fig 4E). Overall, these data suggested that the systemic inflammatory response in MRSA infection was associated with Tlpps, and MRSA Tlpps contributed to bacterial colonization and virulence.

β-lactam-antibiotic-stimulated Tlpps promoted the pathogenesis of MRSA

We determined whether β-lactam-stimulated Tlpps enhanced the pathogenesis of MRSA. A mouse subcutaneous infection model was used to evaluate the contribution of the subinhibitory concentrations of OXA or Tlpps to skin and soft tissue infections. The mice were subcutaneously injected in both flanks with 5×10^7 OXA-treated N315 and N315Δ*tlpps* cells and intraperitoneally injected with 1 μg of OXA per gram weight twice a day for 14 days. The course of infection was monitored every day. The untreated N315- and N315Δ*tlpps*-infected and PBS-injected mice served as the controls. The abscesses caused by the OXA-treated N315 was significantly larger than those caused by the OXA-treated N315Δ*tlpps*, untreated N315, and untreated N315Δ*tlpps* (Fig 5A), and this observation was further shown in the photographs of the skin lesions (Fig 5B and S5 Fig). Histological examinations indicated that the skin of the OXA-treated N315-challenged mice exhibited less extensive inflammation with leukocyte infiltration, destroyed skin structure, and more flake-like abscess-formation than those of the untreated N315-infected and PBS-injected mice (Fig 5C). By contrast, the skin of the OXA-treated N315Δ*tlpps*-challenged mice displayed more leukocyte infiltration and sporadic abscess formation than that of the untreated N315Δ*tlpps*-infected and PBS-injected mice. The corium layer of the N315-challenged and PBS-injected mice showed an extensive inflammation with leukocyte infiltration, although abscess formation was not observed compared with that of the N315Δ*tlpps*-infected and PBS-injected mice. These pathological phenomena might be caused by the β-lactam-stimulated MRSA Tlpps, which stimulated the IL-6 and TNFα levels in mice (Fig 5D and 5E), thereby silencing the

267 immune responses through granulocytic and monocyticmyeloid-derived suppressor
268 cells induced by IL-6 [17], increasing immune cells death due to the tremendous
269 TNFα release [24], and promoting bacterial colonization and abscess formation.
270 Overall, these data confirmed that β-lactam-stimulated Tlpps worsened the MRSA
271 infections.
272
273 **β-lactam-stimulated Tlpp expression in MRSA was SarA dependent**
274 β-lactams as antibiotics block the cell wall synthesis of bacteria to exert antimicrobial
275 effects. By contrast, β-lactams as inductors may trigger global regulatory networks to
276 modulate virulence in *S. aureus* [13]. RT-qPCR revealed that the expression of global
277 regulators, including *sarA*, *agrA*, *RNAIII*, *rot*, *ccpA*, and *saeR*, increased in
278 OXA-treated N315 compared with those in the untreated ones (Fig 6A). *SarA* and
279 *agrA* were the most altered regulators, whereas *sigB* was unchanged, which was
280 consistent with the Western blot results of SigB stimulated with different OXA
281 concentrations (S6 Fig). AgrA is a downstream regulator of SarA [25]. In this study,
282 we examined whether SarA was upregulated in N315 upon OXA treatment. Western
283 blot analysis indicated that both SarA and Tlpps increased in a dose-dependent
284 manner in response to the β-lactam antibiotic treatment (Fig 6B, 6C and S2 Fig). The
285 deletion of *sarA* reduced the Tlpps levels in both N315 and its culture supernatant
286 (Fig 6D and S7 Fig). The *sarA* overexpressing strain (N315Δ*sarA*/pLI-*sarA*)
287 produced even more Tlpps compared with the wild type N315, whereas the empty
288 pLI50 plasmid-carrying strain (N315Δ*sarA*/pLI50) did not. Consistent with the
289 decreased Tlpps in N315Δ*sarA*, N315Δ*sarA* or its culture supernatant stimulated less
290 IL-6 and TNFα expression in RAW264.7 cells than N315 or its culture supernatant
291 did. By contrast, N315Δ*sarA*/pLI-*sarA* or its culture supernatant induced more IL-6
292 and TNFα expression than the wild-type N315 or N315Δ*sarA*/pLI50 did (S8 Fig). The
293 IL-6 and TNFα levels in mice challenged with N315Δ*sarA* decreased compared with
294 those in the mice challenged with N315. N315Δ*sarA*/pLI-*sarA* stimulated even higher
295 cytokine levels in mice compared with those of N315 or N315Δ*sarA* induced (Fig 6E
296 and 6F). Taken together, these data indicated that the β-lactam-stimulated Tlpp

297 expression in MRSA was SarA dependent.

298

299 **SarA directly controlled the β-lactam-stimulated Tlpp expression in MRSA**

300 To investigate the effect of SarA on β-lactam-stimulated Tlpp expression, we
301 constructed a reporter vector (pOS1-*tlpps*^{P}) containing the *tlpp* promoter-controlled
302 *lacZ* gene (S6 Table) and performed β-galactosidase assay by transforming
303 pOS1-*tlpps*^{P} into the MRSA strains N315 and N315Δ*sarA*. The results revealed that
304 the β-galactosidase activity was significantly lower in the *sarA* mutant than that in
305 N315. Moreover, the β-galactosidase activity presented no significant change in the
306 *sarA* mutant after OXA treatment compared with the untreated N315Δ*sarA* (Fig 7A).
307 However, OXA treatment significantly increased the β-galactosidase activity in N315,
308 and this increase was consistent with the increasing Tlpp in MRSA strains (Fig 7A,
309 Fig 1A and 1B). Consistent with the β-galactosidase assay results, Western blot
310 analysis demonstrated that the Tlpp expression in the *sarA* mutant could not respond
311 to β-lactam simulation (Fig 7B and 7C), suggesting that SarA controlled the Tlpp
312 expression in response to the β-lactam antibiotic induction.

313 A global regulator can recognize specific motifs in the promoter regions of a
314 certain gene, thereby controlling the gene expression [13,26,27]. We analyzed the
315 binding motif of SarA [28,29] in the promoter regions of *tlpps* and found a typically
316 predicted SarA box (Fig 7D). The recombinant His-tagged SarA was prepared and
317 purified from *E. coli* (S7C Fig), and the electrophoretic mobility shift assay (EMSA)
318 showed that the recombinant SarA proteins bound to the *tlpp* cluster promoter region
319 that carried the putative SarA binding box (Fig 7 E, 7F and 7H). No shifting band was
320 observed when the AT-rich SarA box was mutated to become GC-rich (Fig 7E, 7G
321 and 7H). These data indicated that *S. aureus* SarA could directly bind to the *tlpp*
322 cluster promoter region, thereby upregulating the *tlpp* expression in the presence of
323 β-lactams. The AT-rich motif (ATTTAAT) in the promoter regions of *tlpps* is
324 essential for SarA binding and regulating.

325

Discussion

MRSA is distinct from MSSA in terms of the acquisition of a genetic element called staphylococcal cassette chromosome *mec* (SCC*mec*) in which *mecA* encodes an alternative penicillin-binding protein 2a (PBP2a) with a low affinity for β-lactams [21]. As such, MRSA strains are resistant to nearly all β-lactam antibiotics [6]. As antibiotics, β-lactams bind to penicillin-binding proteins (PBPs) and inhibit the transpeptidation and transglycosylation of the cell wall, resulting in a weakened cell wall and inducing cell lysis and death [30]. This type of antibiotics, particularly cephalosporins and β-lactam/β-lactamase inhibitor combinations, has been empirically used for clinical treatments of infectious diseases [31]. The subinhibitory concentrations of antistaphylococcal agents might arise because of antibiotic-resistant microorganisms or pharmacokinetics of antibiotics [13,31]. For MRSA infections, which are not initially recognized, β-lactams are not only ineffective in the treatment of infections but also likely contributing to poor outcomes by enhancing the pathogenicity of MRSA. Nonetheless, the underlying mechanisms remain obscure [9]. In this study, we showed that a three-gene constituent *tlpp* cluster upregulated in response to β-lactam induction in a dose- and time-dependent manner. This *tlpp* cluster, belonging to a DUF576 protein family of unknown function [19,22], was widely distributed among the major prevalent MRSA clones (Fig 1B and S4 Table). Tlpps could be upregulated after treatment with nearly all β-lactam antibiotics, such as penicillin (oxacillin and methicillin), cephalosporins (cefoxitin), and carbapenems (imipenem and meropenem), but not with vancomycin, kanamycin, and erythromycin (Fig 1A).

In addition to antimicrobial activity, signal induction may be implemented by the subinhibitory concentrations of β-lactams. They actively promote *S. aureus* biofilm formation [3], induce PBP2a to reduce peptidoglycan crosslinking in MRSA [6], and enhance virulence factors, such as alpha-toxins, PVL, SPA, and enterotoxins [2,32-34]. In contrast to β-lactam-stimulated SPA and PVL, which have a controversial pathogenic role in *S. aureus* [2], the Lpps of *S. aureus* are crucial

355 players in alerting the host immune system by recognizing TLR2/TLR1 or
356 TLR2/TLR6 receptors [24,35]. In general, the Lpps of Gram-positive bacteria are
357 anchored in the outer leaflet of the cytoplasmic membrane [17]. We observed that the
358 β-lactam-stimulated MRSA Tlpps could be released; Tlpps could be detected in both
359 cell lysates and the culture supernatant through Western blot analysis (Fig 2D, 2F, 3C
360 and 3F). MRSA Tlpps could induce the production of IL-6 and TNFα
361 proinflammatory cytokines of macrophages which stimulated with the culture
362 supernatant of N315 post-treated with different OXA concentrations (Fig 3A and 3B).
363 Although the *tlpp* deletion mutant (N315Δ*tlpps*) infection induced less IL-6 and
364 TNFα production in mice compared with the wild-type N315 was administrated,
365 OXA-treated N315Δ*tlpps*-infected mice still produced higher IL-6 and TNFα
366 cytokines compared with those of the untreated N315-challenged mice (Fig 5D and
367 5E), suggesting that other mechanisms might be involved in the immune system
368 modulation by β-lactam-treated MRSA. For instance, β-lactam-promoted PBP2a
369 induction can diminish the peptidoglycan crosslinking, thereby enhancing phagocytic
370 degradation and detection and resulting in strong IL-1β production [6].

371 In addition to stimulating the immune system, increasing the pathogenicity of
372 MRSA was attributed to β-lactam-stimulated Tlpps. In comparison with wild-type
373 N315, the N315Δ*tlpps* strain significantly decreased the bacterial burden in mouse
374 kidneys (Fig 4C, 4D and 4E). β-lactam antibiotic treatment exacerbated MRSA
375 infections in the mouse skin infection model, and the histological examinations of the
376 OXA-treated N315-challenged mouse skin displayed less extensive infiltration with
377 leukocytes, destroyed skin structure, and easily promoted abscess formation (Fig 5). A
378 possible explanation is that the induced IL-6 and TNFα expression by
379 β-lactam-stimulated MRSA Tlpps silenced the innate immune responses [24], thereby
380 facilitating MRSA colonization and infection. Our findings might indicate that MRSA
381 infections were associated with higher morbidity and mortality than MSSA [7,36].

382 β-lactams can induce PVL expression in *S. aureus* by interfering with PBP1 and
383 triggering SarA and Rot global regulators [2]. Our results showed that SarA and AgrA
384 were the most upregulated regulators in MRSA N315 after OXA treatment (Fig 6A).

The deletion of SarA (N315Δ*sarA*) failed to upregulate *tlpps* even under OXA treatment (Fig 7A and 7B), indicating that the β-lactam-induced Tlpp expression in MRSA was SarA controlled. EMSA data revealed that the regulation of SarA on Tlpp expression was direct (Fig 7F). However, further investigations should be performed to clarify how β-lactams trigger the SarA expression.

In conclusion, this work focused on the function and regulation of a new *tlpp* cluster in response to the induction of subinhibitory concentrations of β-lactams. We demonstrated that the increased Tlpps in MRSA significantly enhanced inflammatory response by triggering IL-6 and TNFα levels in vitro and in vivo, thereby possibly contributing to bacterial pathogenicity and worsening the outcome of MRSA infection by reducing host immune responses and promoting bacterial colonization. β-lactam-stimulated MRSA Tlpps was SarA dependent, and the upregulation in Tlpp expression after β-lactam treatment was directly controlled by the global regulator SarA (Fig 8). Nonetheless the pathways leading to the SarA expression trigged by β-lactam antibiotics remain unknown. Our data support the recommendation to clinicians that the discreet usage of β-lactams which possibly worsened the clinical outcome of MRSA infections.

Materials and methods

Ethics statement

BALB/c mice were purchased from Laboratory Animal Center of Army Medical University (Third Military Medical University). All animal experiments were approved by the Army Medical University Institutional Animal Care and Use Committee (protocol #SYXK-PLA-20120031). All animal experimental procedures were performed in accordance with the Regulations for the Administration of Affairs Concerning Experimental Animals approved by the State Council of People`s Republic of China.

414 **Bacterial strains and plasmids**

415 Bacterial strains and plasmids used in this study were listed in S6 Table. *E. coli*
416 strains DH5α and BL21 (DE3) were cultivated in Luria Broth (LB) medium (Oxoid).
417 *S. aureus* strains grown in Brain Heart Infusion (BHI) or Tryptic Soy Broth (TSB)
418 medium (Oxoid).

419

420 **Antibiotic susceptibility tests**

421 Antibiotic susceptibility was determined using broth microdilution methods according
422 to the protocols recommended by the Clinical and Laboratory Standards Institute
423 (CLSI, 2017) [37]. The antibiotic susceptibility results for all strains were listed in S2
424 Table.

425

426 **Preparation of recombinant Tlpp1 and SarA**

427 Recombinant Tlpp1 and SarA proteins were prepared in our laboratory. In brief, the
428 gene encoding for Tlpp1 or SarA was amplified from the genomic DNA of N315 by
429 PCR, and cloned into pET28a(+) vector to construct the pET28a-*tlpp*1 and
430 pET28a-*sarA* plasmids. Then, the recombinant plasmids were transformed into *E. coli*
431 BL21(DE3) for the expression of Tlpp1-6×His and SarA-6×His fusion proteins. Cells
432 were grown in LB with 100 μg/ml of ampicillin at 37 °C.
433 Isopropyl-D-thiogalactopyranoside (IPTG, 5 μM) was added once an OD600 of 0.6
434 was achieved. The cells were cultured at 22 °C for another 6 h. The cells were then
435 centrifuged at 10,000 × g for 15min, washed once with PBS, resuspended in the lysis
436 buffer (50 mM Tris·Cl, 0.15 M NaCl, 1 mM phenylmethanesulfonyl fluoride (PMSF),
437 0.5mg/ml lysozyme, pH 8.0) and lysed using ultrasonic method. The recombinant
438 proteins in the supernatant were purified by Ni-NTA affinity chromatography (GE
439 Healthcare) and identified by Western blot.

440

441 **Preparation of protein-specific polyclonal antibodies**

442 Female BALB/c mice (6–8 weeks) were immunized subcutaneously with 40 μg of
443 recombinant proteins (Tlpp1 or SarA) emulsified with complete Freund's adjuvant

(Sigma, USA) for the first time, and boosted with recombinant proteins (Tlpp1 or SarA) in incomplete Freund's adjuvant on day 14, 28, and 35, respectively. Seven days after the last immunization, blood samples were collected, the titer of antibodies against Tlpp1 or SarA was determined by ELISA.

Preparation of the total bacteria proteins and the culture supernatant proteins

Overnight MRSA culture was diluted 1:100 in BHI medium with or without the addition of β-lactam antibiotics, cultivated at 37 °C to an optical density (OD) at 600 nm of 2.0. Then, bacterial cells in 3 ml culture were harvested by centrifugation at 10,000 × g at 4 °C. The cell pellets were washed twice with PBS, resuspended in 1 ml of cold PBS supplemented with 1% β-mercaptoethanol (Sigma, USA) and 1 mM PMSF (Beyotime, China) on ice. Cells were broken by the addition of 0.1-mm diameter zirconia/silica beads, shaking on the Minibeadbeater 16 instrument (Biospec, USA). Cell debris was removed after centrifugation at 10,000 × g for 10 min at 4 °C, and the total cell proteins in 1 ml of the supernatant were precipitated with 7.5% trichloroacetic acid (TCA)/0.2 % deoxycholic acid solution.

The culture supernatant of MRSA stimulated with or without antibiotics was harvested by centrifugation at 10,000 × g for 10 min at 4 °C. The proteins in 1 ml culture supernatant were prepared by TCA precipitation, collected by centrifugation at 15,000 × *g* for 10 min, washed once with ice-cold acetone, dissolved in 60 μl of PBS for use. The protein concentration was determined using the Bradford Protein Assay Kit (Beyotime, China).

Proteomic analysis

LC-MS/MS was performed to identify proteins induced by β-lactam antibiotics as previously described [38]. MRSA strain N315 was cultured in TSB with or without 2 μg/ml OXA. The total bacteria proteins were separated through SDS–PAGE, and the antibiotic-induced protein band was excised and analyzed through LC-MS/MS by using UltiMate3000 RSLCnano liquid chromatography/Bruker maxis 4G Q-TOF. The resulting peptide mass fingerprints were compared against the ORFs of N315 by using

Mascot and Mascot Daemon software (Matrix Science).

RT-PCR and RT-qPCR

Total MRSA N315 RNA was extracted as previously described [39]. Overnight N315 cultures were 1:100 diluted in TSB containing 2 μg/ml OXA, cultivated at 37 °C to the early exponential phase (OD600 = 1.0). Total RNA was isolated using the TriPure isolation reagent (Roche Applied Science, Germany) after the collected cells were firstly lysed using lysostaphin (Sigma, USA). cDNA was synthesised from 500 ng of total RNA using gene-specific primers and a RevertAid First Strand cDNA Synthesis Kit (Thermo, USA). RT-PCR was used to test whether *tlpp1*, *tlpp2*, and *tlpp3* were cotranscribed. RT-qPCR was performed to detect the expression levels of the *tlpp* genes (*tlpp*1, *tlpp*2 and *tlpp*3) and the global regulators (*sarA*, *agrA*, *RNAIII*, *rot*, *ccpA*, *saeR*, *sigB*) using SsoAdvanced™ Universal SYBR® Green Supermix (Bio-Rad, USA). The relative expression level of all tested genes was normalized to that of the 16S *rRNA*. All primers used are listed in S5 Table.

Construction of gene mutant strains

The *tlpp* cluster marker-less deletion mutant was constructed using homologous recombinant strategy described previously [39]. Briefly, the *tlpp* cluster deletion plasmid pYT3-Δ*tlpps* (S3A Fig) was constructed by amplifying the upstream and downstream regions of *tlpp* cluster with primer pairs, up-*tlpps* fwd/up-*tlpps* rev and down-*tlpps* fwd/down-*tlpps* rev, and subcloning these fragments into *E. coli*-*S. aureus* temperature-sensitive shuttle vector pYT3. The recombinant plasmid was identified by DNA sequencing and subsequently transformed into RN4220 by electroporation, then transformed into N315. The resulting N315Δ*tlpps* strain was generated after inducing the integration of plasmid into chromosome at 42 ℃ and following inducing the plasmid losing at 25 ℃. The deletion of *tlpp* cluster was confirmed by PCR and DNA sequencing.

To construct the *tlpps* complementary strain, the *tlpp* cluster containing its potential promoter region was amplified by pLI-*tlpps* fwd/pLI-*tlpps* rev primer pairs,

cloned into the expression plasmid pLI50 [40]. Then, the correctly constructed plasmid pLI-*tlpps* was electroporated into RN4220 and then N315Δ*tlpps* to generate N315Δ*tlpp*/pLI-*tlpps* strain. Similar strategy was used to construct N315Δ*sarA*/pLI-*sarA*. The empty pLI50 plasmid transformed N315Δ*tlpps* and N315Δ*sarA* strains served the controls. All primers used are listed in S5 Table.

Cytokine determination

RAW264.7 (TIB-71™, ATCC) cells were cultured in high glucose DMEM (Thermo Fisher Scientific, USA) added 10 % (v/v) fetal bovine serum (Thermo Fisher Scientific, USA) at 37 ℃ with 5 % CO_2. For stimulation experiment, RAW264.7 cells (10^6/well) were either infected with MRSA strain (MOI of 30), or cultured in DMEM medium containing 5% (v/v) bacterial culture supernatant, in a 24-well microtiter plate for 6 h as described [41]. Then, the supernatant was collected, and the levels of IL-6 and TNFα were measured with an ELISA kit following the manufacturer's instructions (R&D Systems, USA).

To detect the ability of Tlpp proteins in inducing cytokine secretion in vivo, female BALB/c mice were infected via tail vein injection with 1×10^7 CFU of N315, N315Δ*tlpps*, N315Δ*tlpps*/ pLI-*tlpps*, N315Δ*tlpps*/pLI50, N315Δ*sarA*, N315Δ*sarA*/pLI-*sarA*, and N315Δ*sarA*/pLI50, respectively. Blood samples were collected 6 h post infection, and the IL-6 and TNFα levels in mouse sera were determined by using ELISA.

Animal experiments

BALB/c mice were randomly divided into two groups and infected via tail vein injection with 1×10^7 CFU of the GFP-expression plasmid (pGFP) transformed N315 or N315Δ*tlpps*, sacrificed 5 days after infection. Mouse organs (i.e., heart, lung, liver, spleen, and kidney) were isolated and subjected to the determination of GFP fluorescence efficiency in the organs with IVIS® Lumina LT system and analyzed by Living Image 4.4 Software. The bacterial loads in the infected kidneys were also counted via plate dilution assay as described [42].

For skin abscess formation, BALB/c mice were fully anesthetized with 1 % pentobarbital sodium (50 mg/kg) and the back hair was depilated completely with 6 % sodium sulfide (w/v). Then, mice were subcutaneously inoculated with 5×10^7 CFU of MRSA N315 and N315Δ*tlpps* in both flanks of the murine back as described [43], and then randomly divided into two groups. The mice of the treatment group were intraperitoneally injected with 1 μg of OXA per gram weight twice a day for 14 days. The PBS-injected mice served as the controls. The abscess area assessed by the maximal length × width of the developing ulcer was measured daily.

For histopathological examination, the skin lesions were fixed by 4 % paraformaldehyde, paraffin embed, and stained with hematoxylin & eosin (H&E).

β-galactosidase assay

A *tlpp* promoter-LacZ reporter plasmid (pOS1-*tlpps*^{P}) was constructed by inserting the *tlpp* promoter region into pOS1 vector, and transformed into N315 and N315Δ*sarA*, respectively. Then, pOS1-*tlpps*^{P}-carried N315 and N315Δ*sarA* were cultured overnight, diluted 1:100 in BHI, and cultivated at 37 ℃ to an OD600 of 0.6. Bacterial cells in 200 μl culture were collected by centrifugation, suspended in 100 μl of AB buffer (100 mM KH_2PO_4, 100 mM NaCl, pH 7.0), and treated with lysostaphin (20 μg/ml, Sigma) for 15 min at 37 ℃. Then, the suspension was added with another 900 μl of ABT solution (AB buffer containing 0.1 % TritonX-100) [44], 50 μl of the solution was mixed with 10 μl of MUG (4-methylumbelliferyl-β-D-galactoside, 4 mg/mL, Sigma) and incubated for 1 h at room temperature. Then, 20 μL of the sample was mixed with 180 μl of ABT solution, and the reaction was monitored at 445 nm with an excitation wavelength of 365 nm. All samples were tested in triplicate. The LacZ activity was normalized to the cell density of OD600, and the relative activity was calculated by setting the LacZ activity from the N315 to 100%. The assay was repeated at least three times.

Electrophoretic mobility shift assays (EMSA)

The predicted *tlpp* cluster promoter, an AT-rich motif fragment (56 bp), was

564 synthesized using the primer pairs (EMSA-*tlpps*^{P} fwd/EMSA-*tlpps*^{P} rev) as described
565 [45]. The corresponding mutated GC-rich motif fragment was also synthesized by
566 primer pairs EMSA-*tlpps*^{PM} fwd/EMSA-*tlpps*^{PM} rev and served as the control. Ten
567 picomole of DNA fragment was incubated with a variable amount of recombinant
568 SarA (0 to 240 pM) in a 20 μl reaction mixture containing 10 mM HEPES (pH 7.6), 1
569 mM EDTA, 2 mM dithiothreitol, 50 mM KCl, 0.05 % Triton X-100, and 5 %
570 glycerol. Binding reactions were equilibrated for 20 min at room temperature before
571 electrophoresis. Reaction mixtures were separated on 6 % native polyacrylamide gel
572 electrophoresis in 0.5 × TBE (Tris/boric acid/EDTA) buffer at 90 V for 2 h at 4 ℃.
573 Gels were stained by GelRed dye (Biotium, USA) and observed under UV light. The
574 primers used are listed in S5 Table .
575
576 **Statistical analysis**
577 Statistical analysis was carried out using GraphPad Prism 6.0. Unpaired two-tailed
578 student's t-test, analysis of variance (ANOVA) and Mann-Whitney test were used
579 appropriately to compare the difference between groups. Each experiment was carried
580 out at least three times. Results were presented as mean ± standard deviations (S.D.),
581 and a P value less than 0.05 was considered statistically significant. * $P < 0.05$, ** P
582 < 0.01, *** $P < 0.001$, and ns represented no significance.
583

584 ## Supporting Information

585 **S1 Fig. Alignment of the tandem lipoproteins (Tlpps).** (A) Alignment of the Tlpp1,
586 Tlpp2, and Tlpp3 signal peptide and the lipobox sequence. (B) Alignment of the
587 Tlpp1, Tlpp2, and Tlpp3 proteins. The amino acid sequences of the indicated protein
588 were retrieved from UniProt (http://www.uniprot.org/), and the alignment was
589 conducted through the BioEdit program. The identical amino acids were colored.
590 (TIF)
591 **S2 Fig. Western blot analysis of Tlpps and SarA in N315 with different**
592 **concentrations of MET treatment.** (A) Tlpps and SarA upregulated in N315 with

MET treatment in a dose-dependent manner. The molecular weights of the protein marker (M) were indicated on the left. LC, loading control. (B) Evaluation of gray value of the N315 Tlpps and SarA in each lane using ImageJ software. The relative value of Tlpps or SarA/loading control (LC) in the first lane (0 μg/ml MET) was adjusted to 1.0, and the relative gray values in other lanes were calculated and indicated.

(TIF)

S3 Fig. Construction of N315Δ*tlpps* and N315Δ*tlpps*/pLI-*tlpps* strains. (A) Schematics for construction of the *tlpp* marker-less deletion plasmid pYT3-Δ*tlpps* and the complementation plasmid pLI-*tlpps*. (B) Identification of N315Δ*tlpps* by PCR using primer pairs *c_tlpps fwd*/*c_tlpps rev* (S5 Table). (C) Identification of N315Δ*tlpps* by DNA sequencing.

(TIF)

S4 Fig. The recombinant Tlpp1 proteins presented no effect on IL-6 and TNFα expression by macrophages. (A) IL-6 and (B) TNFα levels produced by macrophages post-treated with the recombinant Tlpp1 proteins of 200 ng, 400 ng, or 600 μg were given. The cytokine levels were determined by ELISA after 6 h post-treated. LPS (200 ng) administrated was served as the positive control, and PBS-treated served as the negative control. The experiments were conducted in thrice. *** $P < 0.001$.

(TIF)

S5 Fig. Abscesses in mice 7 days after infection. The mice were subcutaneously injected in both flanks with 5×10^7 OXA-treated N315 and N315Δ*tlpps* cells and intraperitoneally injected with 1 μg of OXA per gram weight twice a day for 14 days. The skin lesions were recorded at the 7en day post-infection. The abscesses caused by the OXA-treated N315 were larger than those caused by the OXA-treated N315Δ*tlpps*, PBS-treated N315, and PBS-treated N315Δ*tlpps*.

(TIF)

S6 Fig. Western blot analysis of SigB in N315 with different concentrations of OXA treatment. (A) SigB was not changed in N315 with OXA treatment. The

623 molecular weights of the protein marker (M) were indicated on the left. LC, loading
624 control. (B) Evaluation of gray value of the N315 SigB in each lane using ImageJ
625 software. The relative value of SigB/LC in the first lane (0 μg/ml OXA) was adjusted
626 to 1.0, and the relative gray values in other lanes were calculated and indicated.
627 (TIF)

628 **S7 Fig. The deletion of *sarA* decreased the secretory Tlpp expression by N315.**
629 (A) Western blot analysis of the reduced expression of Tlpp proteins in the culture
630 supernatant of N315Δ*tlpps*, which could be restored by the complementary *sarA*
631 (N315Δ*sarA*/pLI-*sarA*) but not by the empty pLI50 plasmid-carrying strain
632 (N315Δ*sarA*/pLI50). LC, loading control. (B) Evaluation of gray value of the Tlpp
633 proteins in each lane using ImageJ software. The relative value of Tlpp/LC in the first
634 lane (N315) was adjusted to 1.0, and the relative gray values in other lanes were
635 calculated and indicated. (C) SDS-PAGE analysis of the recombinant SarA
636 (His-tagged).
637 (TIF)

638 **S8 Fig. SarA mutant stimulated less IL-6 and TNFα production in macrophages.**
639 (A) IL-6 and (B) TNFα levels produced by macrophages post-treated with the culture
640 supernatant of N315, N315Δ*sarA*, N315Δ*sarA*/pLI-*sarA*, and N315Δ*sarA*/pLI50,
641 respectively. (C) IL-6 and (D) TNFα levels produced by macrophages infected with
642 N315, N315Δ*sarA*, N315Δ*sarA*/pLI-*sarA*, and N315Δ*sarA*/pLI50 at an MOI of 30.
643 The cytokine levels were determined by ELISA 6 h post-infection. The experiments
644 in duplicate were conducted in thrice. ns represented no statistical significance, * $P <$
645 0.05, ** $P < 0.01$, *** $P < 0.001$.
646 (TIF)

647 **S9 Fig. Growth curve of MRSA strain N315 in the culture media containing**
648 **different concentrations of OXA as indicated.** Independent growth rates of different
649 concentrations of OXA treated N315 were determined. The experiment was
650 conducted in thrice, and the data were shown as mean ± S.D. The growth of MRSA
651 N315 was significantly inhibited by more than 4 μg/ml of OXA was administrated at
652 the early stage, although the MIC value of N315 against OXA was higher as 512

μg/ml (S2 Table) because of the heterogeneous β-lactam-resistant phenotype of MRSA [46]. Therefore, the subinhibitory concentrations of OXA, 2 μg/ml, was used unless specifically stated in this study.

(TIF)

S10 Fig. Full Western blot data. The full-length blots for all Western blot pictures. The black boxes represented the depicted parts of the blot.

(TIF)

S1 Table. Predicted Lpps of *S. aureus* N315.

(DOCX)

S2 Table. The MICs of MRSA strains.

(DOCX)

S3 Table. Proteins identified in the protein band of β-lactams induced MRSA N315 by LC-MS/MS.

(DOCX)

S4 Table. The distribution of *tlpps* cluster in major MRSA clones.

(DOCX)

S5 Table. Primers used in this study.

(DOCX)

S6 Table. Strains and plasmids used in this work.

(DOCX)

Acknowledgments

We would like to thank the members of the Xiancai Rao and Xuhu Mao research groups for their critical reading of the manuscript. We thank Professor Baolin Sun (University of Science and Technology of China) providing plasmid pGFP and pLI50. We also thank Professor Lefu Lan (Shanghai Institute of Materia Medica, Chinese Academy of Sciences) for providing plasmid pOS1.

References

682 1. Gutierrez A, Laureti L, Crussard S, Abida H, Rodriguez-Rojas A, et al. (2013)
683 beta-Lactam antibiotics promote bacterial mutagenesis via an RpoS-mediated
684 reduction in replication fidelity. Nat Commun 4: 1610. PMID:23511474.
685 2. Dumitrescu O, Choudhury P, Boisset S, Badiou C, Bes M, et al. (2011)
686 Beta-lactams interfering with PBP1 induce Panton-Valentine leukocidin
687 expression by triggering *sarA* and *rot* global regulators of *Staphylococcus*
688 *aureus*. Antimicrob Agents Chemother 55: 3261-3271. PMID:21502633.
689 3. Kaplan JB, Izano EA, Gopal P, Karwacki MT, Kim S, et al. (2012) Low levels of
690 beta-lactam antibiotics induce extracellular DNA release and biofilm
691 formation in *Staphylococcus aureus*. MBio 3: e00198-00112.
692 PMID:22851659.
693 4. Lowy FD (1998) *Staphylococcus aureus* infections. N Engl J Med 339: 520-532.
694 PMID:9709046.
695 5. Liu H, Shang W, Hu Z, Zheng Y, Yuan J, et al. (2018) A novel SigB(Q225P)
696 mutation in *Staphylococcus aureus* retains virulence but promotes biofilm
697 formation. Emerging microbes & infections 7: 72. PMID:29691368.
698 6. Muller S, Wolf AJ, Iliev ID, Berg BL, Underhill DM, et al. (2015) Poorly
699 Cross-Linked Peptidoglycan in MRSA Due to *mecA* Induction Activates the
700 Inflammasome and Exacerbates Immunopathology. Cell Host Microbe 18:
701 604-612. PMID:26567511.
702 7. Antonanzas F, Lozano C, Torres C (2015) Economic features of antibiotic
703 resistance: the case of methicillin-resistant *Staphylococcus aureus*.
704 Pharmacoeconomics 33: 285-325. PMID:25447195.
705 8. Barrios Lopez M, Gomez Gonzalez C, Orellana MA, Chaves F, Rojo P (2013)
706 *Staphylococcus aureus* abscesses: methicillin-resistance or Panton-Valentine
707 leukocidin presence? Arch Dis Child 98: 608-610. PMID:23728388.
708 9. Watkins RR, David MZ, Salata RA (2012) Current concepts on the virulence
709 mechanisms of meticillin-resistant *Staphylococcus aureus*. J Med Microbiol
710 61: 1179-1193. PMID:22745137.
711 10. Paul M, Kariv G, Goldberg E, Raskin M, Shaked H, et al. (2010) Importance of

712 appropriate empirical antibiotic therapy for methicillin-resistant
713 *Staphylococcus aureus* bacteraemia. J Antimicrob Chemother 65: 2658-2665.
714 PMID:20947620.
715 11. Kim SH, Park WB, Lee KD, Kang CI, Bang JW, et al. (2004) Outcome of
716 inappropriate initial antimicrobial treatment in patients with
717 methicillin-resistant *Staphylococcus aureus* bacteraemia. J Antimicrob
718 Chemother 54: 489-497. PMID:15254028.
719 12. Kernodle DS, McGraw PA, Barg NL, Menzies BE, Voladri RK, et al. (1995)
720 Growth of *Staphylococcus aureus* with nafcillin in vitro induces alpha-toxin
721 production and increases the lethal activity of sterile broth filtrates in a murine
722 model. J Infect Dis 172: 410-419. PMID:7542686.
723 13. Hodille E, Rose W, Diep BA, Goutelle S, Lina G, et al. (2017) The Role of
724 Antibiotics in Modulating Virulence in *Staphylococcus aureus*. Clin Microbiol
725 Rev 30: 887-917. PMID:28724662.
726 14. Nielsen LN, Roggenbuck M, Haaber J, Ifrah D, Ingmer H (2012) Diverse
727 modulation of *spa* transcription by cell wall active antibiotics in
728 *Staphylococcus aureus*. BMC Res Notes 5: 457. PMID:22920188.
729 15. Shahmirzadi SV, Nguyen MT, Gotz F (2016) Evaluation of *Staphylococcus*
730 *aureus* Lipoproteins: Role in Nutritional Acquisition and Pathogenicity. Front
731 Microbiol 7: 1404. PMID:27679612.
732 16. Hutchings MI, Palmer T, Harrington DJ, Sutcliffe IC (2009) Lipoprotein
733 biogenesis in Gram-positive bacteria: knowing when to hold 'em, knowing
734 when to fold 'em. Trends Microbiol 17: 13-21. PMID:19059780.
735 17. Nguyen MT, Gotz F (2016) Lipoproteins of Gram-Positive Bacteria: Key Players
736 in the Immune Response and Virulence. Microbiol Mol Biol Rev 80: 891-903.
737 PMID:27512100.
738 18. Babu MM, Priya ML, Selvan AT, Madera M, Gough J, et al. (2006) A database of
739 bacterial lipoproteins (DOLOP) with functional assignments to predicted
740 lipoproteins. J Bacteriol 188: 2761-2773. PMID:16585737.
741 19. Nguyen MT, Kraft B, Yu W, Demircioglu DD, Hertlein T, et al. (2015) The νSaα

Specific Lipoprotein Like Cluster (*lpl*) of *S. aureus* USA300 Contributes to Immune Stimulation and Invasion in Human Cells. PLoS Pathog 11: e1004984. PMID:26083414.

20. Nguyen MT, Hanzelmann D, Hartner T, Peschel A, Gotz F (2016) Skin-Specific Unsaturated Fatty Acids Boost the *Staphylococcus aureus* Innate Immune Response. Infect Immun 84: 205-215. PMID:26502910.

21. Cheng H, Yuan W, Zeng F, Hu Q, Shang W, et al. (2013) Molecular and phenotypic evidence for the spread of three major methicillin-resistant *Staphylococcus aureus* clones associated with two characteristic antimicrobial resistance profiles in China. J Antimicrob Chemother 68: 2453-2457. PMID:23766485.

22. Schluepen C, Malito E, Marongiu A, Schirle M, McWhinnie E, et al. (2013) Mining the bacterial unknown proteome: identification and characterization of a novel family of highly conserved protective antigens in *Staphylococcus aureus*. Biochem J 455: 273-284. PMID:23895222.

23. Rogero MM, Calder PC (2018) Obesity, Inflammation, Toll-Like Receptor 4 and Fatty Acids. Nutrients 10. PMID:29601492.

24. Nguyen MT, Uebele J, Kumari N, Nakayama H, Peter L, et al. (2017) Lipid moieties on lipoproteins of commensal and non-commensal staphylococci induce differential immune responses. Nat Commun 8: 2246. PMID:29269769.

25. Reyes D, Andrey DO, Monod A, Kelley WL, Zhang G, et al. (2011) Coordinated regulation by AgrA, SarA, and SarR to control agr expression in *Staphylococcus aureus*. J Bacteriol 193: 6020-6031. PMID:21908676.

26. Peacock SJ, Paterson GK (2015) Mechanisms of Methicillin Resistance in *Staphylococcus aureus*. Annu Rev Biochem 84: 577-601. PMID:26034890.

27. Arya R, Princy SA (2013) An insight into pleiotropic regulators Agr and Sar: molecular probes paving the new way for antivirulent therapy. Future Microbiol 8: 1339-1353. PMID:24059923.

28. Liu Y, Manna AC, Pan CH, Kriksunov IA, Thiel DJ, et al. (2006) Structural and

772 function analyses of the global regulatory protein SarA from *Staphylococcus*
773 *aureus*. Proc Natl Acad Sci U S A 103: 2392-2397. PMID:16455801.
774 29. Sterba KM, Mackintosh SG, Blevins JS, Hurlburt BK, Smeltzer MS (2003)
775 Characterization of *Staphylococcus aureus* SarA binding sites. J Bacteriol 185:
776 4410-4417. PMID:12867449.
777 30. Lim D, Strynadka NC (2002) Structural basis for the beta lactam resistance of
778 PBP2a from methicillin-resistant *Staphylococcus aureus*. Nat Struct Biol 9:
779 870-876. PMID:12389036.
780 31. Wushouer H, Tian Y, Guan XD, Han S, Shi LW (2017) Trends and patterns of
781 antibiotic consumption in China's tertiary hospitals: Based on a 5 year
782 surveillance with sales records, 2011-2015. PLoS One 12: e0190314.
783 PMID:29281716.
784 32. Ohlsen K, Ziebuhr W, Koller KP, Hell W, Wichelhaus TA, et al. (1998) Effects of
785 subinhibitory concentrations of antibiotics on alpha-toxin (*hla*) gene
786 expression of methicillin-sensitive and methicillin-resistant *Staphylococcus*
787 *aureus* isolates. Antimicrob Agents Chemother 42: 2817-2823.
788 PMID:9797209.
789 33. Kuroda H, Kuroda M, Cui L, Hiramatsu K (2007) Subinhibitory concentrations of
790 beta-lactam induce haemolytic activity in *Staphylococcus aureus* through the
791 SaeRS two-component system. FEMS Microbiol Lett 268: 98-105.
792 PMID:17263851.
793 34. Subrt N, Mesak LR, Davies J (2011) Modulation of virulence gene expression by
794 cell wall active antibiotics in *Staphylococcus aureus*. J Antimicrob Chemother
795 66: 979-984. PMID:21393149.
796 35. Hashimoto M, Tawaratsumida K, Kariya H, Aoyama K, Tamura T, et al. (2006)
797 Lipoprotein is a predominant Toll-like receptor 2 ligand in *Staphylococcus*
798 *aureus* cell wall components. Int Immunol 18: 355-362. PMID:16373361.
799 36. Ganga R, Riederer K, Sharma M, Fakih MG, Johnson LB, et al. (2009) Role of
800 SCCmec type in outcome of *Staphylococcus aureus* bacteremia in a single
801 medical center. J Clin Microbiol 47: 590-595. PMID:19144813.

802 37. CLSI. Performance Standards for Antimicrobial Susceptibility Testing, 27th
803 Edn.Wayne, PA: CLSI (2017).
804 38. Yuan J, Yang J, Hu Z, Yang Y, Shang W, et al. (2018) Safe Staphylococcal
805 Platform for the Development of Multivalent Nanoscale Vesicles against Viral
806 Infections. Nano letters 18: 725-733. PMID:29253342.
807 39. Yuan W, Hu Q, Cheng H, Shang W, Liu N, et al. (2013) Cell wall thickening is
808 associated with adaptive resistance to amikacin in methicillin-resistant
809 *Staphylococcus aureus* clinical isolates. J Antimicrob Chemother 68:
810 1089-1096. PMID:23322605.
811 40. You Y, Xue T, Cao L, Zhao L, Sun H, et al. (2014) *Staphylococcus aureus*
812 glucose-induced biofilm accessory proteins, GbaAB, influence biofilm
813 formation in a PIA-dependent manner. Int J Med Microbiol 304: 603-612.
814 PMID:24836943.
815 41. Curry H, Alvarez GR, Zwilling BS, Lafuse WP (2004) Toll-like receptor 2
816 stimulation decreases IFN-γ receptor expression in mouse RAW264.7
817 macrophages. J Interferon Cytokine Res 24: 699-710. PMID:15684737.
818 42. Burts ML, Williams WA, DeBord K, Missiakas DM (2005) EsxA and EsxB are
819 secreted by an ESAT-6-like system that is required for the pathogenesis of
820 *Staphylococcus aureus* infections. Proc Natl Acad Sci U S A 102: 1169-1174.
821 PMID:15657139.
822 43. Wen W, Liu B, Xue L, Zhu Z, Niu L, et al. (2018) Autoregulation and Virulence
823 Control by the Toxin-Antitoxin System SavRS in *Staphylococcus aureus*.
824 Infect Immun 86. PMID:29440365.
825 44. Sun F, Li C, Jeong D, Sohn C, He C, et al. (2010) In the *Staphylococcus aureus*
826 two-component system sae, the response regulator SaeR binds to a direct
827 repeat sequence and DNA binding requires phosphorylation by the sensor
828 kinase SaeS. J Bacteriol 192: 2111-2127. PMID:20172998.
829 45. Correa EM, De Tullio L, Velez PS, Martina MA, Argarana CE, et al. (2013)
830 Analysis of DNA structure and sequence requirements for *Pseudomonas*
831 *aeruginosa* MutL endonuclease activity. J Biochem 154: 505-511.

PMID:23969026.

46. Aiba Y, Katayama Y, Hishinuma T, Murakami-Kuroda H, Cui L, et al. (2013) Mutation of RNA polymerase beta-subunit gene promotes heterogeneous-to-homogeneous conversion of beta-lactam resistance in methicillin-resistant *Staphylococcus aureus*. Antimicrob Agents Chemother 57: 4861-4871. PMID:23877693.

Figure Captions

Fig 1. Tlpps upregulated in MRSA post-treated with the subinhibitory concentrations of antibiotics. (A) The proteins of different antibiotic-induced MRSA N315 were separated through SDS-PAGE and stained with Coomassie brilliant blue. An untreated N315 served as the negative control, and the molecular weights of the protein marker were indicated on the left. The upregulated protein bands upon β-lactam antibiotic treatment were denoted by yellow triangles. (B) Other major clinically prevalent MRSA strains represented by sequence type (ST) were cultured in the absence or presence of OXA (2 μg/ml, unless specifically stated, S2 Table and S9 Fig). SDS-PAGE was then performed. The yellow triangles indicated that certain upregulated protein bands were similar to those of β-lactam-induced MRSA N315 (ST5). (C) SDS-PAGE analysis of the recombinant Tlpp1 proteins. (D) Western blot analysis of β-lactam-induced proteins in N315. The full-length blot was presented in S10 Fig.

(TIF)

Fig 2. Tlpp genes were co-transcribed and upregulated by OXA in a dose- and time-dependent manner. (A) Genetic organization of the *tlpp* cluster in MRSA N315 genome and the location of primers designed for RT-PCR. (B) *tlpp1*, *tlpp2*, and *tlpp3* were co-transcribed tested by RT-PCR. Agarose gel electrophoresis analysis of PCR products amplified with the genomic DNA, reverse-transcribed cDNA, and RNA as templates. (C) RT-qPCR detection of the expression level of *tlpp1, tlpp2,* and *tlpp3* in N315 with or without OXA treatment was administered. ** $P < 0.01$. (D) Western

blot analysis of the Tlpp levels in N315 total cell lysates after different concentrations of OXA treatment was administered. The molecular weights of the protein marker (M) were indicated on the left. LC, loading control. (E) Evaluation of gray value of the N315 Tlpps in each lane using ImageJ software. The relative value of Tlpps/loading control (LC) in the first lane (0 μg/ml OXA) was adjusted to 1.0, and the relative gray values in other lanes were calculated and indicated. (F) Western blot analysis of the Tlpp levels in N315 culture supernatant (CS) after different concentrations of OXA treatment was administered. (G) Evaluation of gray value of Tlpps in N315 culture supernatant. (H) Western blot analysis of the Tlpp levels in N315 after OXA treatment was administered with time indicated. (I) Evaluation of gray value of Tlpps in N315 after OXA treatment was given with time indicated.

(TIF)

Fig 3. Antibiotic-induced MRSA Tlpps stimulated proinflammatory cytokine production by macrophages. IL-6 (A) and TNFα (B) levels increased by macrophages stimulated by 5% culture supernatant (CS) of N315 treated with different concentrations of OXA as indicated for 6 h. The cell culture of TSB stimulated cells served as the negative control. (C) Western blot analysis of the Tlpp proteins in N315Δ*tlpp*s and N315Δ*tlpp*s/pLI-*tlpps*. Wild type N315 and N315Δ*tlpp*s/pLI-50 served as the controls. IL-6 (D) and TNFα (E) levels elevated by macrophages stimulated with N315, N315Δ*tlpps*, N315Δ*tlpp*/pLI-*tlpps*, and N315Δ*tlpps*/pLI50 at the MOI of 30. (F) Western blot analysis of the Tlpp proteins in the culture supernatant of N315Δ*tlpp*s and N315Δ*tlpp*s/pLI-*tlpps*. IL-6 (G) and TNFα (H) levels increased by macrophages treated with 5% culture supernatant (CS) of N315, N315Δ*tlpps*, N315Δ*tlpp*/pLI-*tlpps*, and N315Δ*tlpps*/pLI50, respectively. The experiments were conducted in triplicate. ns represented no statistical significance, * $P < 0.05$, ** $P < 0.01$, *** $P < 0.001$.

(TIF)

Fig 4. Tlpps contributed to the inflammatory response and bacterial colonization in MRSA infection. IL-6 (A) and TNFα (B) levels in mouse sera determined by ELISA. BALB/c mice were infected by tail vein injection with 1×10^7 of N315,

N315Δ*tlpps*, N315Δ*tlpps*/pLI-*tlpps,* and N315Δ*tlpps*/pIL50, respectively. The levels of IL-6 and TNFα in mouse sera were determined 6 h post-infection. Number of mice used, $n = 3$. Phosphate-buffered saline (PBS, pH 7.2) served as the negative control. (C) Organ distribution of N315 and N315Δ*tlpps.* BALB/c mice were infected with 1×10^7 pGFP plasmid transformed N315 and N315Δ*tlpps*, the radiant efficiency of the indicated organs was measured with IVIS® Lumina LT system. (D) Tlpps contributed to the MRSA colonization. The radiant efficiency of N315-infected organs was higher than that of N315Δ*tlpps*-infected ones. (E) Bacterial loads in kidney. BALB/c mice ($n = 7$ for each group) were respectively infected with 1×10^7 of N315 and N315Δ*tlpps* for 5 days, bacteria were recovered and counted from kidneys. ns represented no significance, * $P < 0.05$, ** $P < 0.01$.

(TIF)

Fig 5. β-lactam treatment enhanced the pathogenesis of MRSA in the mouse subcutaneous infection model. (A) Mice were injected subcutaneously with 5×10^7 bacterial cells. Abscess areas were measured daily. (B) Representative abscesses 7 days after infection. (C) Representative histological examinations (H&E stain) of the infected mouse skin. IL-6 (D) and TNFα (E) levels in mouse sera determined by ELISA. BALB/c mice were infected by tail vein injection with 1×10^7 of N315, OXA-treated N315, and OXA-treated N315Δ*tlpps*, respectively. The levels of IL-6 and TNFα in mouse sera were determined 6 h post-infection. Number of mice used, $n = 3$. PBS and OXA served as the controls. ns represented no significance, * $P < 0.05$, ** $P < 0.01$, *** $P < 0.001$.

(TIF)

Fig 6. SarA affected the Tlpp expression in MRSA. (A) RT-qPCR detection of the expression levels of global regulators in MRSA with or without OXA treatment. The expression of each gene in N315 was normalized to that of the 16S *rRNA* gene and adjusted to 1.0, the relative expressions of regulators in OXA-treated N315 were indicated. The experiments were repeated for three times. (B) Western blot analysis of SarA and Tlpp proteins in N315 treated with different concentrations of OXA. (C) Evaluation of gray value of Tlpp and SarA in N315 after OXA treatment. (D) The

921 deletion of *sarA* decreased the Tlpp expression in the N315. SarA mutant stimulated
922 less IL-6 (E) and TNFα (F) production in mice. Mice were infected with 1×10^7 of
923 N315, N315Δ*sarA*, N315Δ*sarA* /pLI-*sarA*, and N315Δ*sarA*/pLI50. The levels of IL-6
924 and TNFα in mouse sera were determined by ELISA 6 h post-infection. The
925 experiments in duplicate were conducted for three times. ns represented no statistical
926 significance, * $P < 0.05$, ** $P < 0.01$, *** $P < 0.001$.
927 (TIF)

928 **Fig 7. SarA bound to the *tlpp* cluster promoter region to control the**
929 **β-lactam-stimulated Tlpp expression in MRSA.** (A) β-galactosidase assay. The
930 pOS1-*tlpps*^{P} reporter plasmid was transformed into N315 and N315Δ*sarA*,
931 respectively. The LacZ activity was detected and represented as mean ± S.D. ($n = 3$).
932 ns indicated no significance, ***$P < 0.001$. (B) SarA controlled β-lactam-stimulated
933 Tlpp expression in N315. (C) Evaluation of gray value of Tlpps and SarA in N315
934 and N315Δ*sarA* with or without OXA treatment. (D) Predicted SarA box in the
935 promoter regions of the *tlpp* cluster. (E) Mutation of AT-rich in the *tlpp* SarA box for
936 EMSA experiment. (F) EMSA. Interaction between wild-type *tlpp* promoter region
937 (*tlpps*-P) and SarA proteins was detected. (G) EMSA with *tlpp* promoter mutant
938 (*tlpps*-PM). (H) Evaluation of gray value of the free probe in each lane using ImageJ
939 software. The value of free probe in the first lane (0 μg protein) was adjusted to 1.0,
940 and the relative gray values in other lanes were calculated and indicated.
941 (TIF)

942 **Fig 8. Schematic of the Tlpp function and its upregulation in MRSA after**
943 **β-lactam treatment.**
944 (TIF)

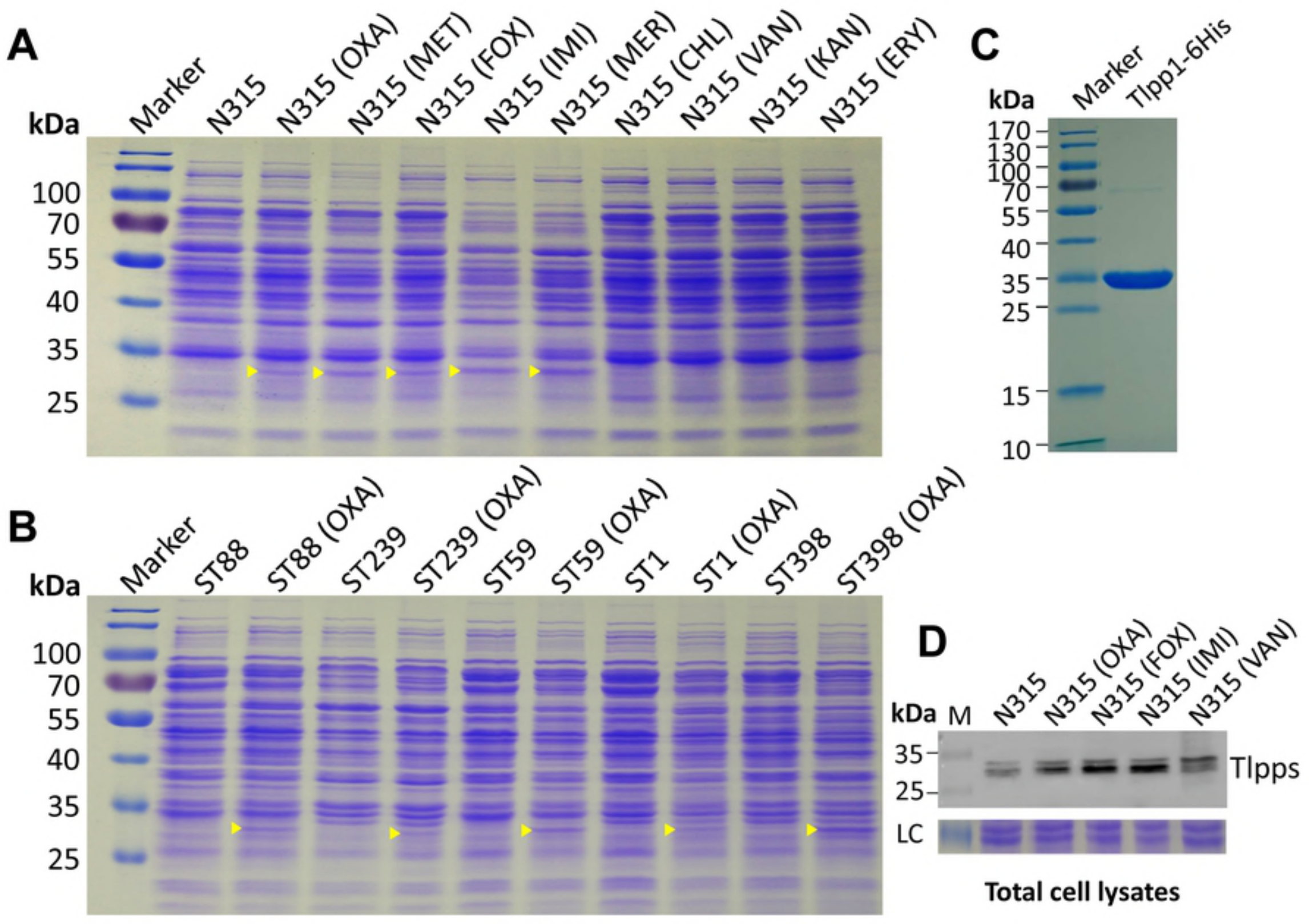
A
kDa
Marker
N315
N315 (OXA)
N315 (MET)
N315 (FOX)
N315 (IMI)
N315 (MER)
N315 (CHL)
N315 (VAN)
N315 (KAN)
N315 (ERY)
100
70
55
40
35
25
B
kDa
Marker
ST88
ST88 (OXA)
ST239
ST239 (OXA)
ST59
ST59 (OXA)
ST1
ST1 (OXA)
ST398
ST398 (OXA)
100
70
55
40
35
25
C
kDa
Marker
Tlpp1-6His
170
130
100
70
55
40
35
25
15
10
D
kDa
M
N315
N315 (OXA)
N315 (FOX)
N315 (IMI)
N315 (VAN)
35
25
Tlpps
LC
Total cell lysates

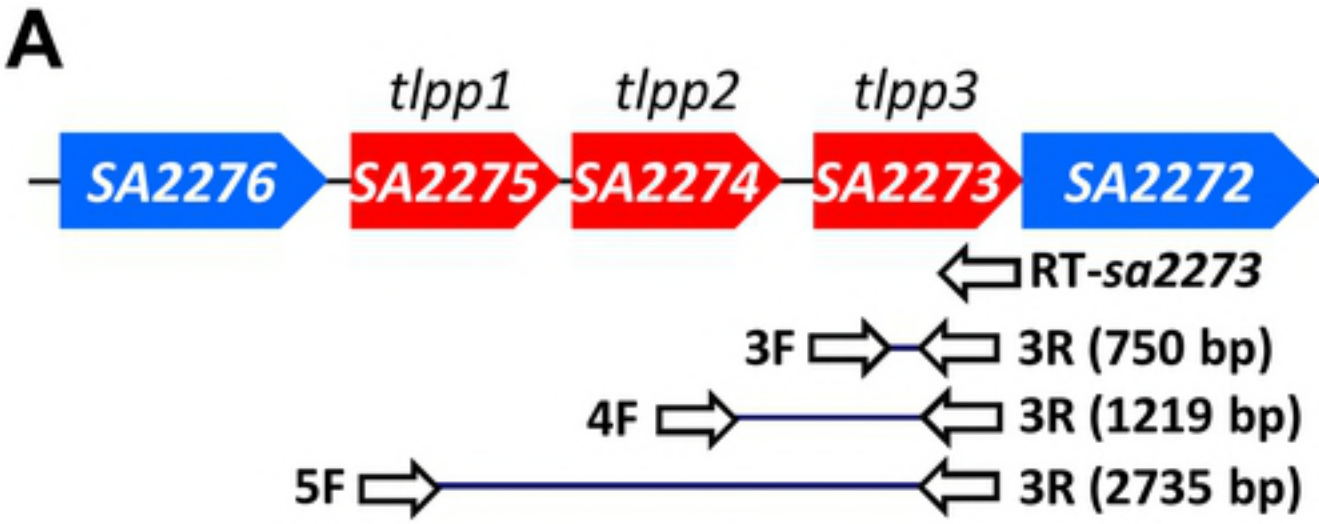
A
tlpp1
tlpp2
tlpp3
SA2276
SA2275
SA2274
SA2273
SA2272
RT-sa2273
3F
3R (750 bp)
4F
3R (1219 bp)
5F
3R (2735 bp)

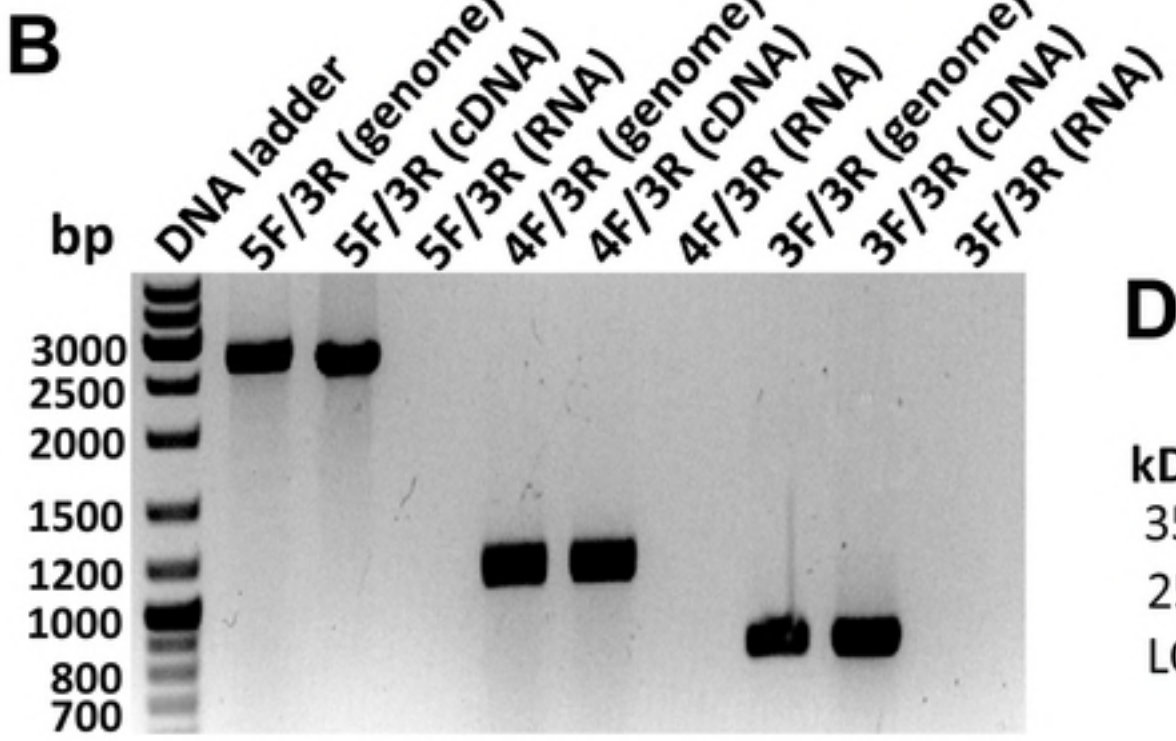
B
bp
DNA ladder
5F/3R (genome)
5F/3R (cDNA)
5F/3R (RNA)
4F/3R (genome)
4F/3R (cDNA)
4F/3R (RNA)
3F/3R (genome)
3F/3R (cDNA)
3F/3R (RNA)
3000
2500
2000
1500
1200
1000
800
700

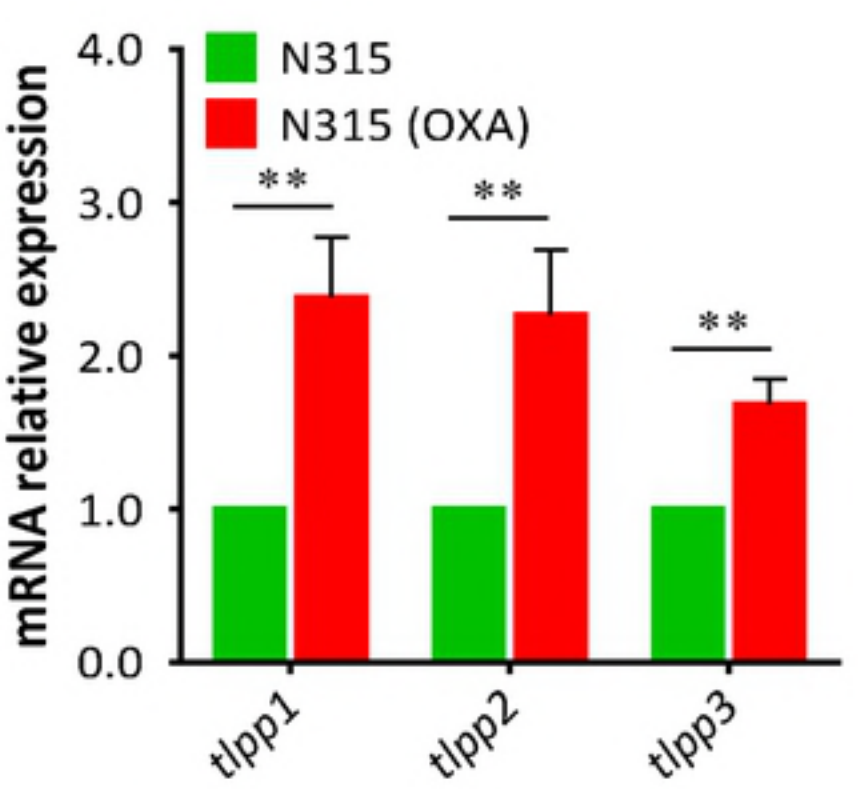
C
N315
N315 (OXA)
mRNA relative expression
4.0
3.0
2.0
1.0
0.0
**
**
**
tlpp1
tlpp2
tlpp3

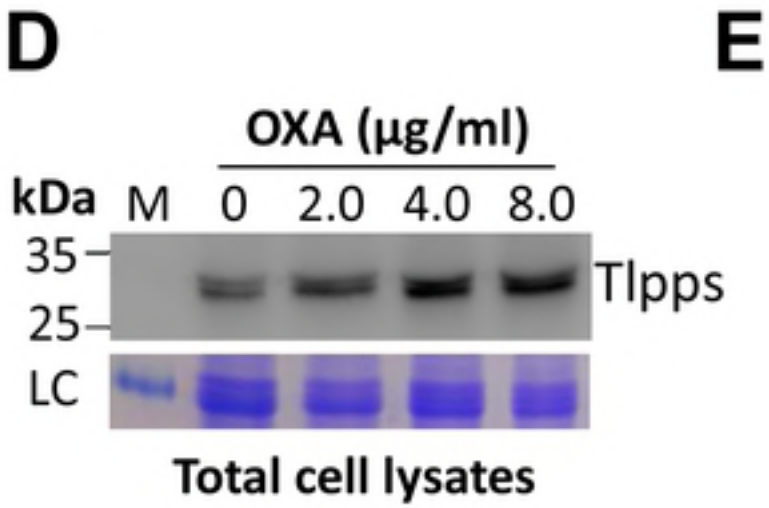
D
OXA (μg/ml)
kDa
M
0
2.0
4.0
8.0
35
25
Tlpps
LC
Total cell lysates

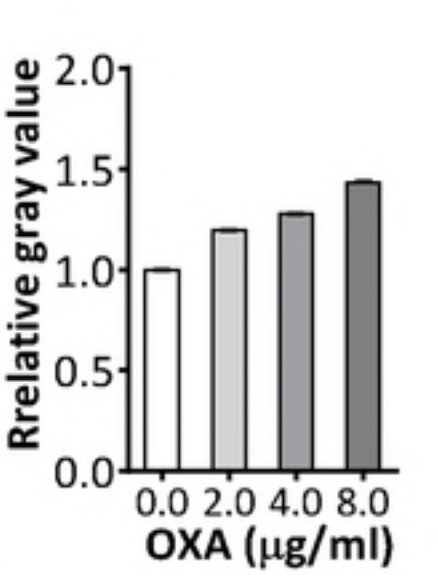
E
Rrelative gray value
2.0
1.5
1.0
0.5
0.0
0.0 2.0 4.0 8.0
OXA (μg/ml)

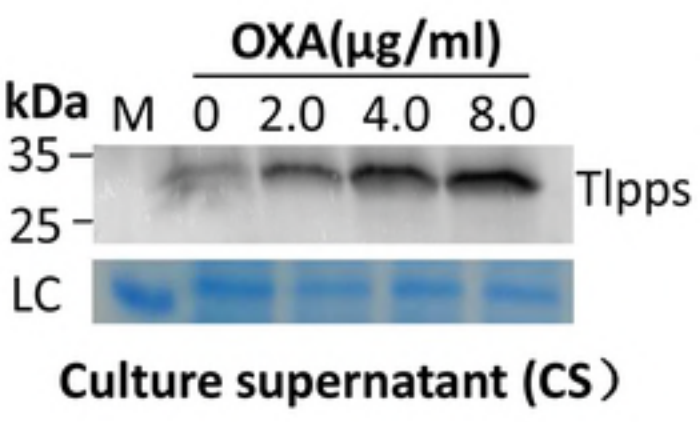
F
OXA(μg/ml)
kDa
M
0
2.0
4.0
8.0
35
25
Tlpps
LC
Culture supernatant (CS）

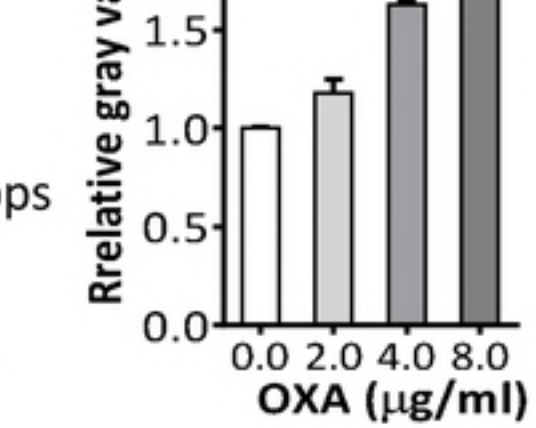
G
Rrelative gray value
2.0
1.5
1.0
0.5
0.0
0.0 2.0 4.0 8.0
OXA (μg/ml)

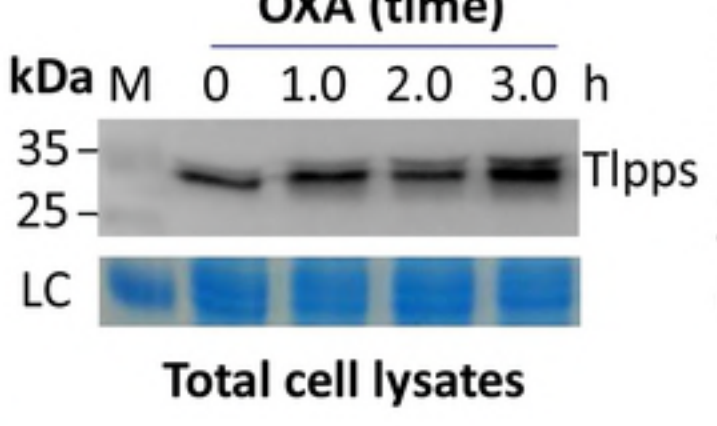
H
OXA (time)
kDa
M
0
1.0
2.0
3.0
h
35
25
Tlpps
LC
Total cell lysates

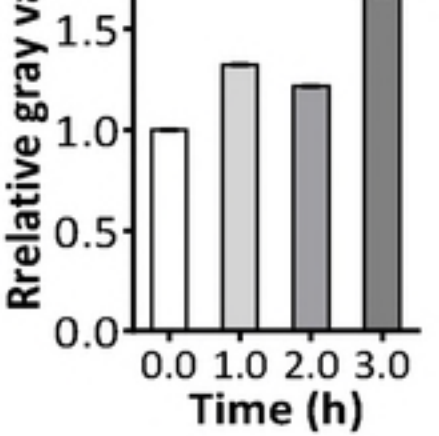
I
Rrelative gray value
2.0
1.5
1.0
0.5
0.0
0.0 1.0 2.0 3.0
Time (h)

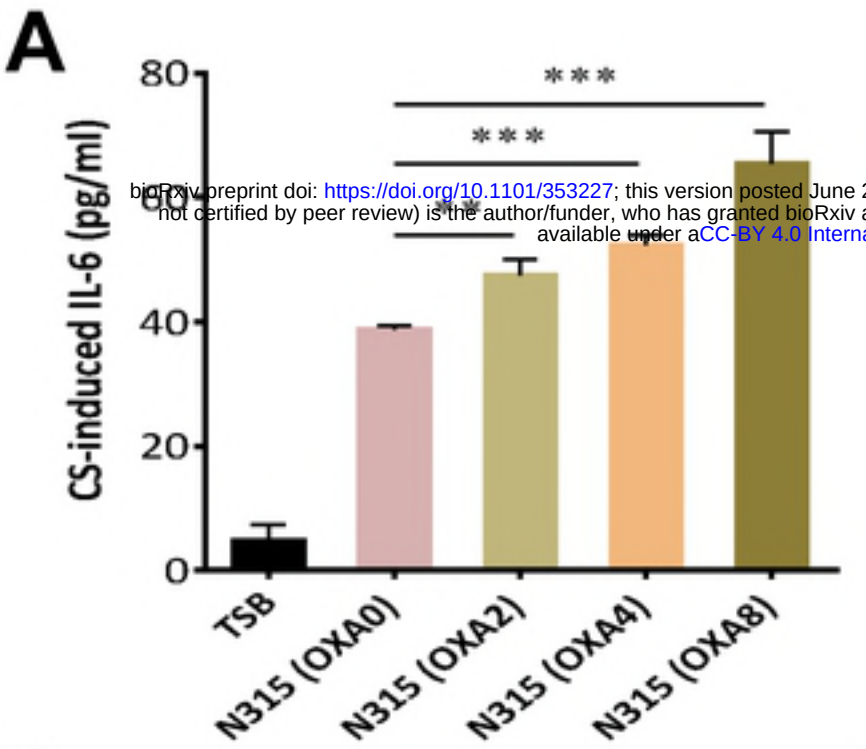

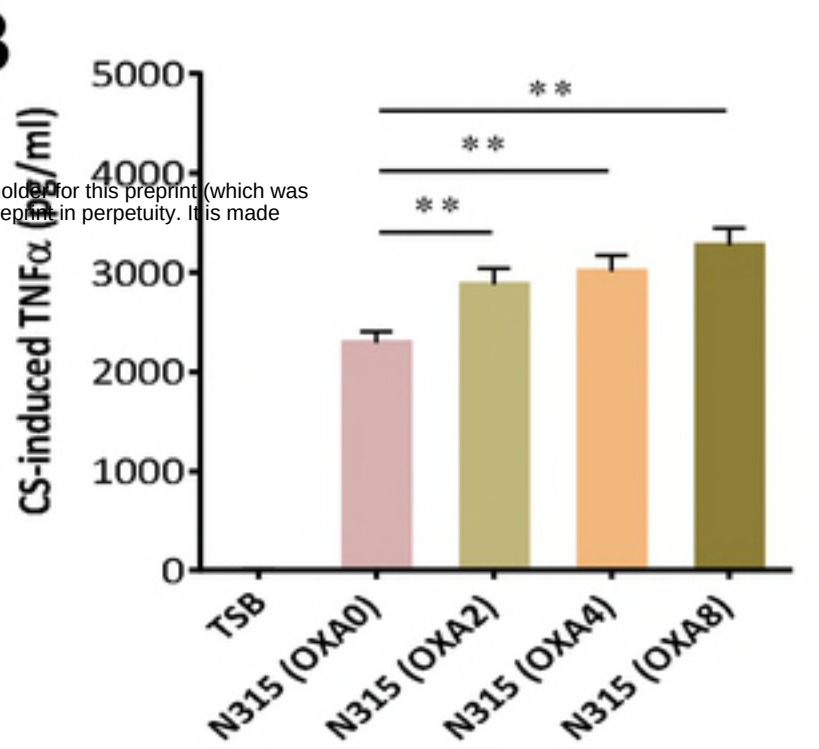

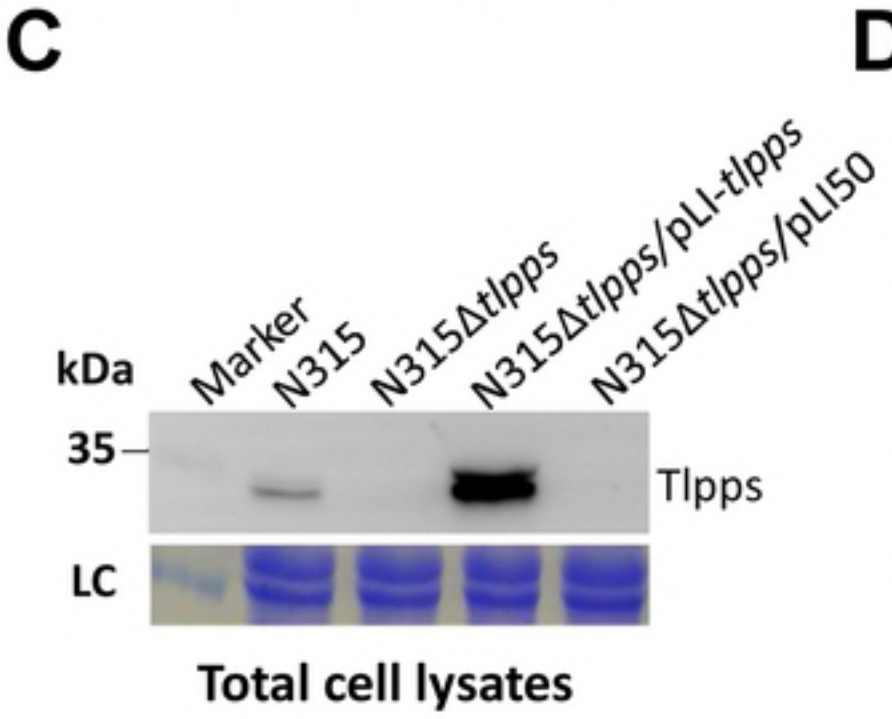

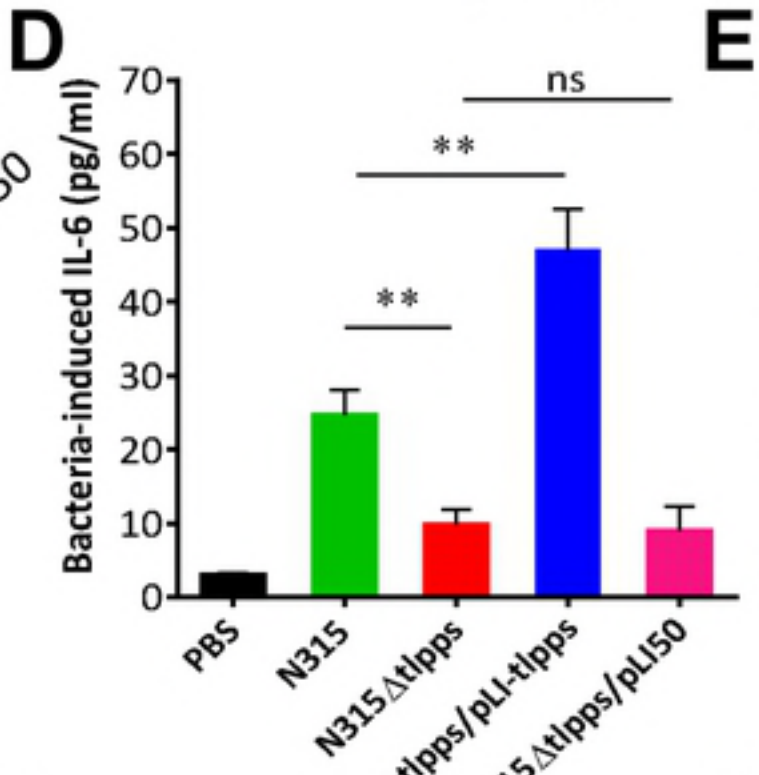

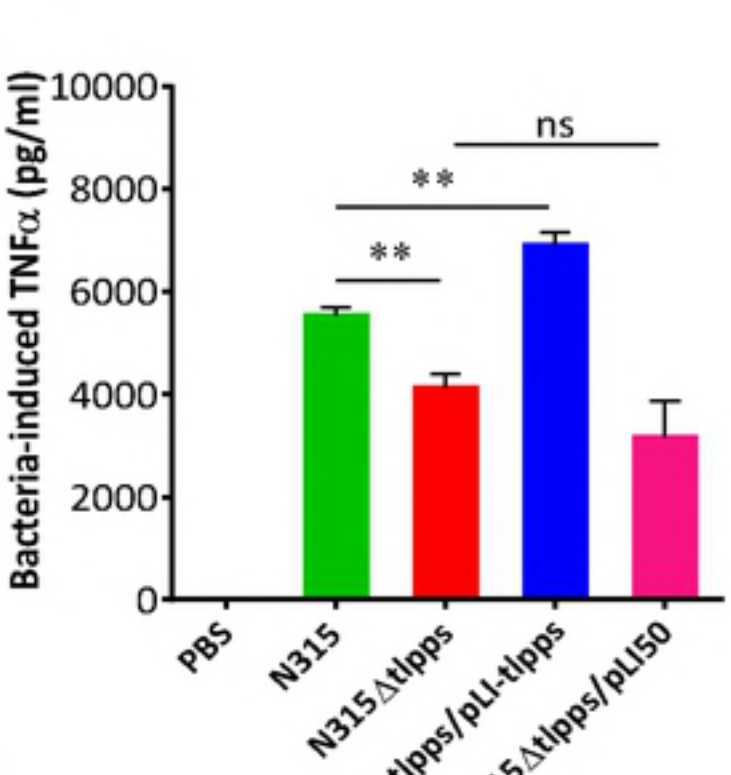

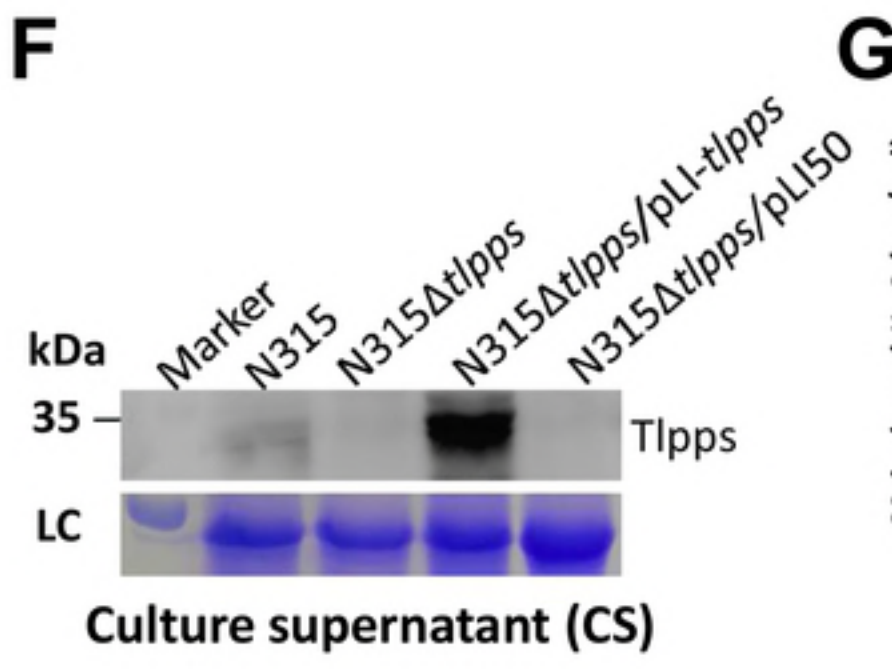

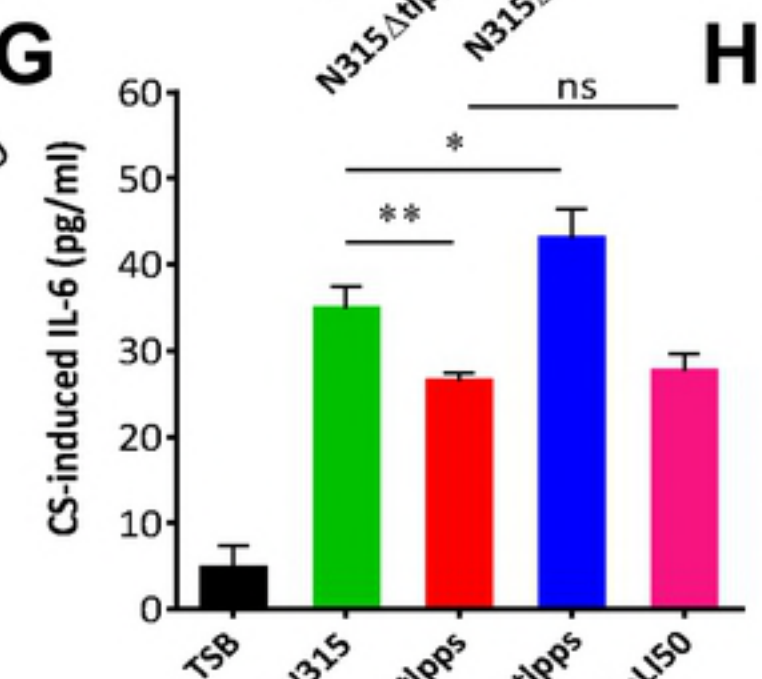

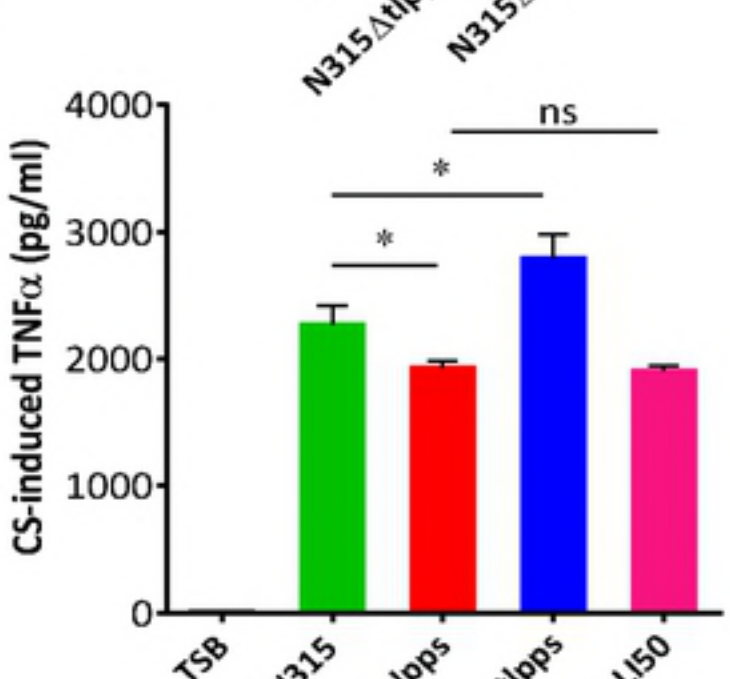

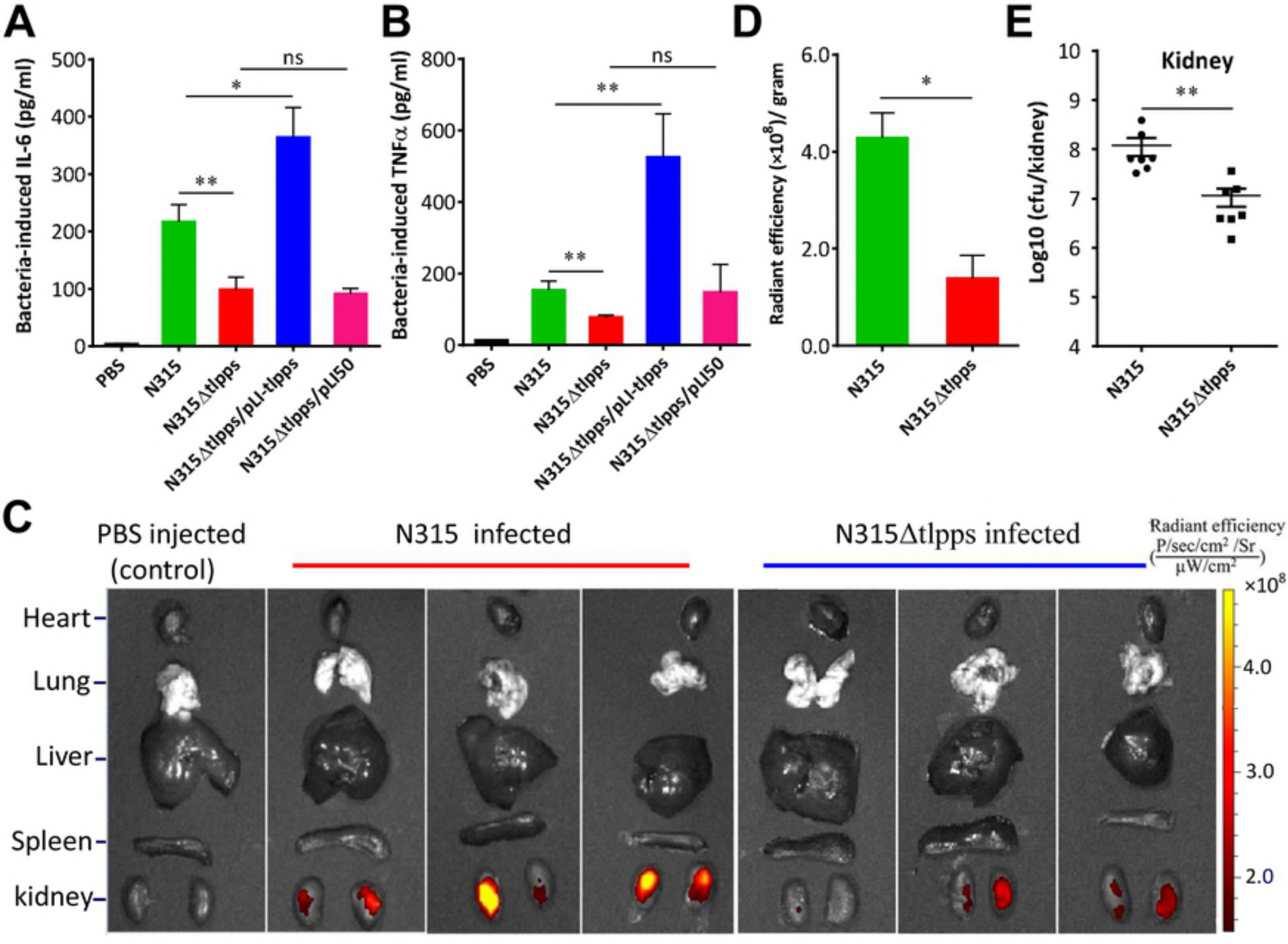
A
Bacteria-induced IL-6 (pg/ml)
500
400
300
200
100
0
ns
*
**
PBS
N315
N315ΔtlppS
N315ΔtlppS/pLI-tlpps
N315ΔtlppS/pLI50
B
Bacteria-induced TNFα (pg/ml)
800
600
400
200
0
ns
**
**
PBS
N315
N315ΔtlppS
N315ΔtlppS/pLI-tlpps
N315ΔtlppS/pLI50
D
Radiant efficiency (×10^8)/ gram
6.0
4.0
2.0
0.0
*
N315
N315ΔtlppS
E
Kidney
Log10 (cfu/kidney)
10
9
8
7
6
5
4
**
N315
N315ΔtlppS
C
PBS injected (control)
N315 infected
N315Δtlpps infected
Radiant efficiency (P/sec/cm² /Sr / μW/cm²)
×10^8
4.0
3.0
2.0
Heart
Lung
Liver
Spleen
kidney

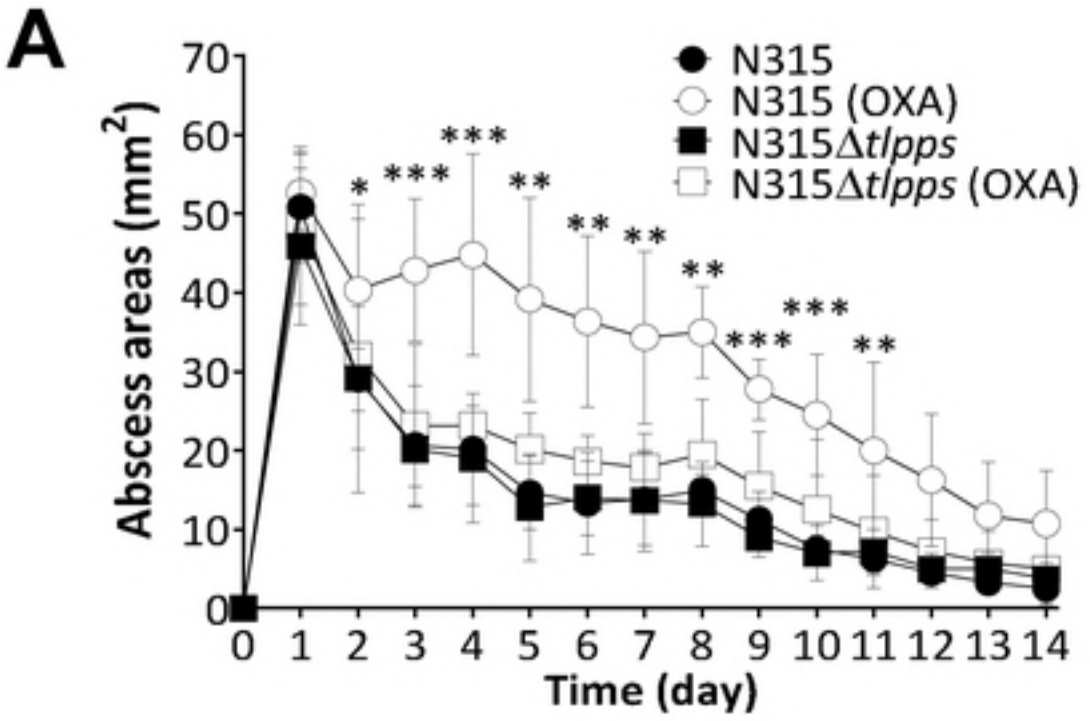

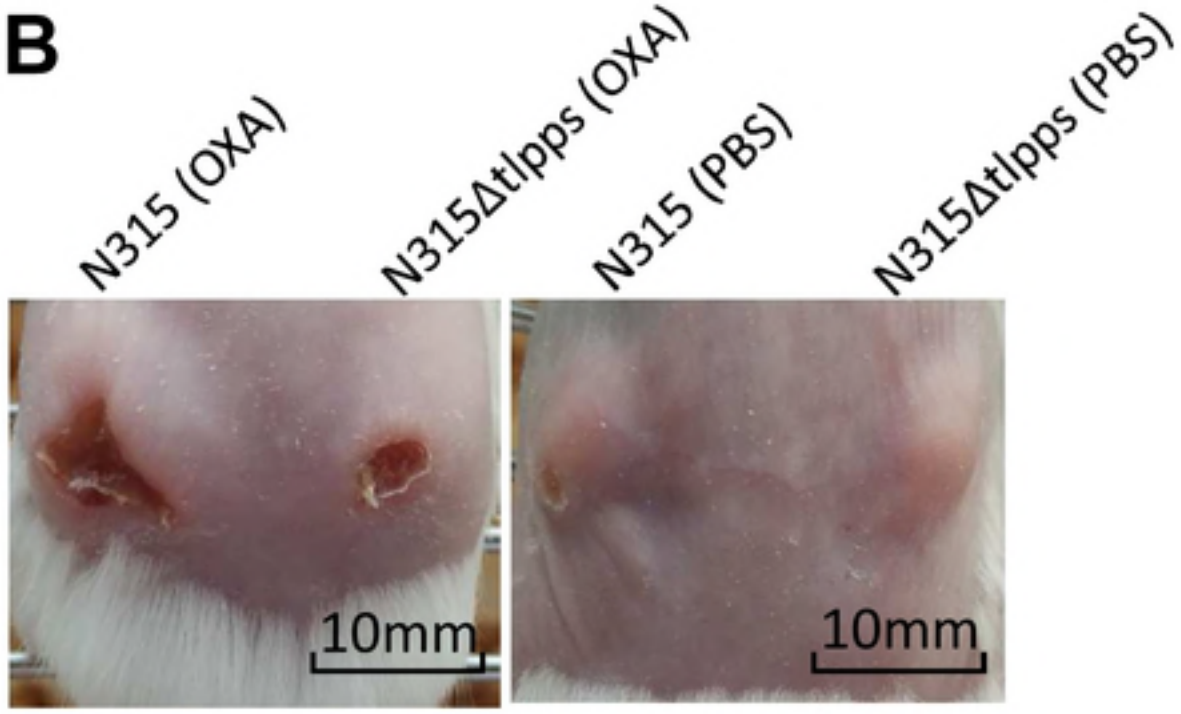

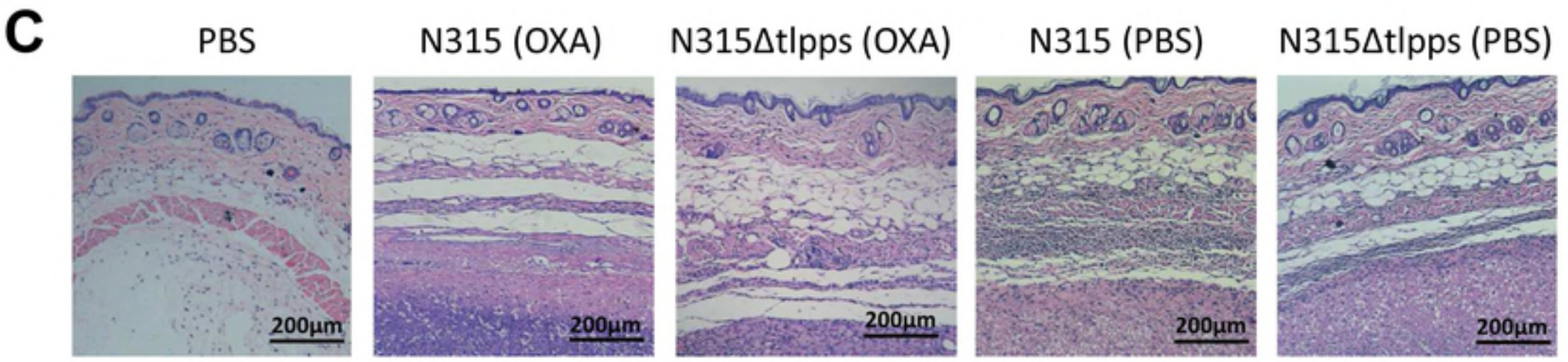

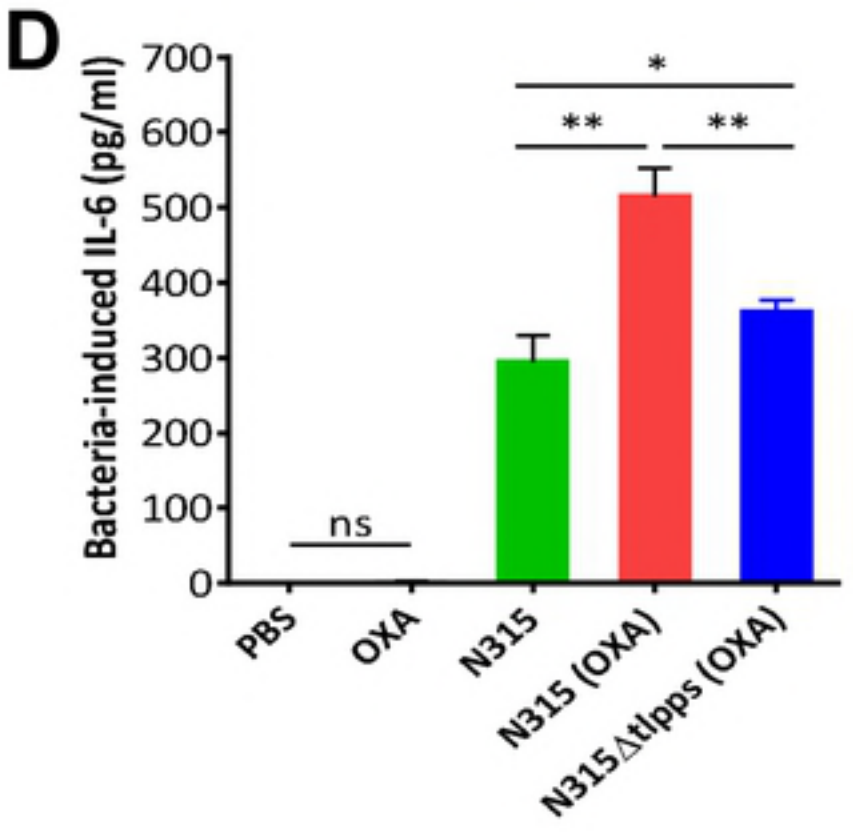

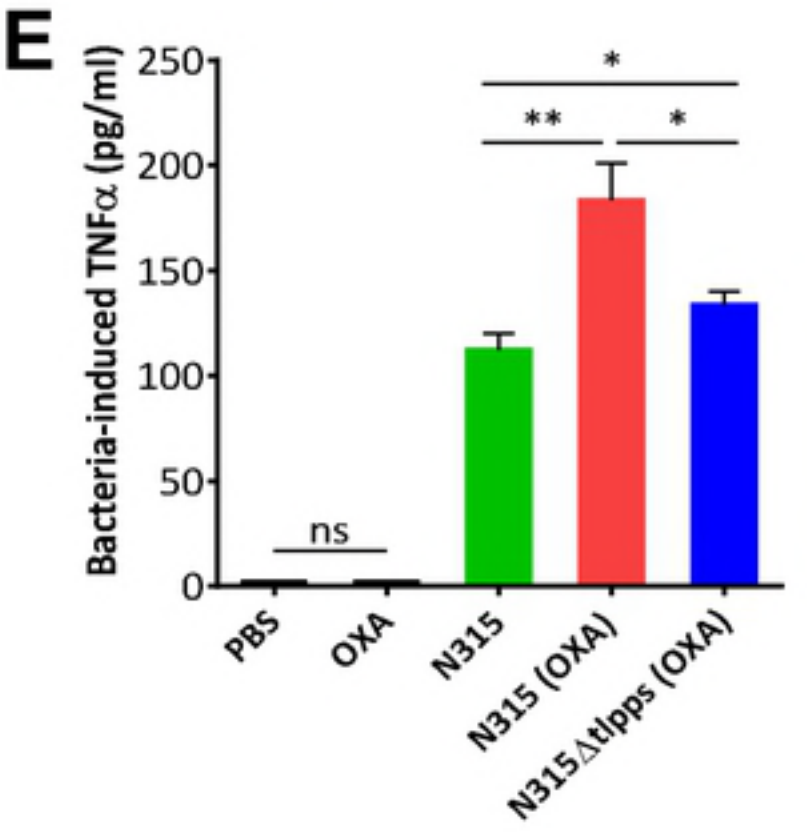

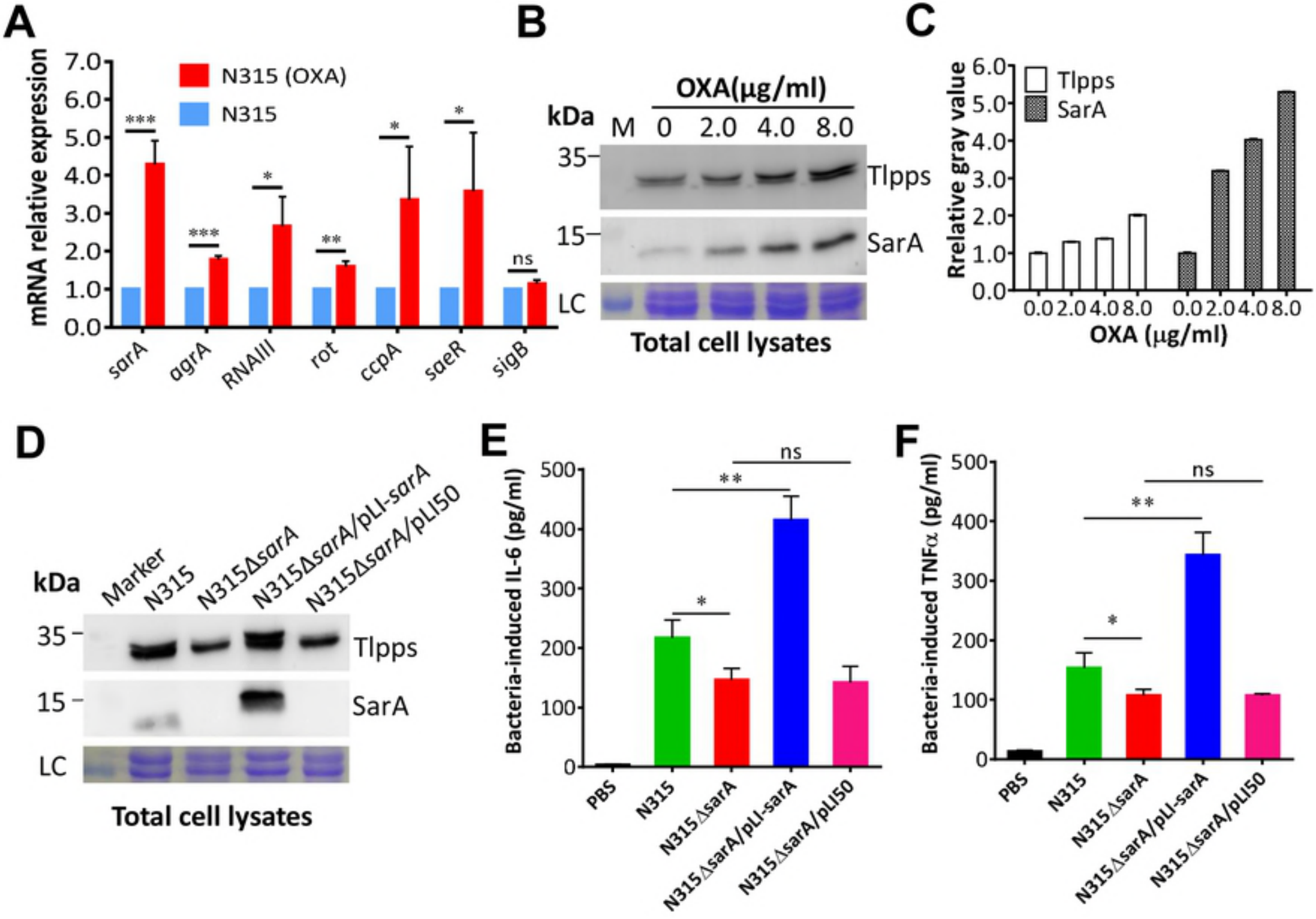
A
mRNA relative expression
N315 (OXA)
N315
sarA
agrA
RNAIII
rot
ccpA
saeR
sigB
B
OXA(μg/ml)
kDa
M
0
2.0
4.0
8.0
35
15
LC
Tlpps
SarA
Total cell lysates
C
Rrelative gray value
Tlpps
SarA
OXA (μg/ml)
D
kDa
Marker
N315
N315ΔsarA
N315ΔsarA/pLI-sarA
N315ΔsarA/pLI50
Tlpps
SarA
LC
Total cell lysates
E
Bacteria-induced IL-6 (pg/ml)
PBS
N315
N315ΔsarA
N315ΔsarA/pLI-sarA
N315ΔsarA/pLI50
F
Bacteria-induced TNFα (pg/ml)

A

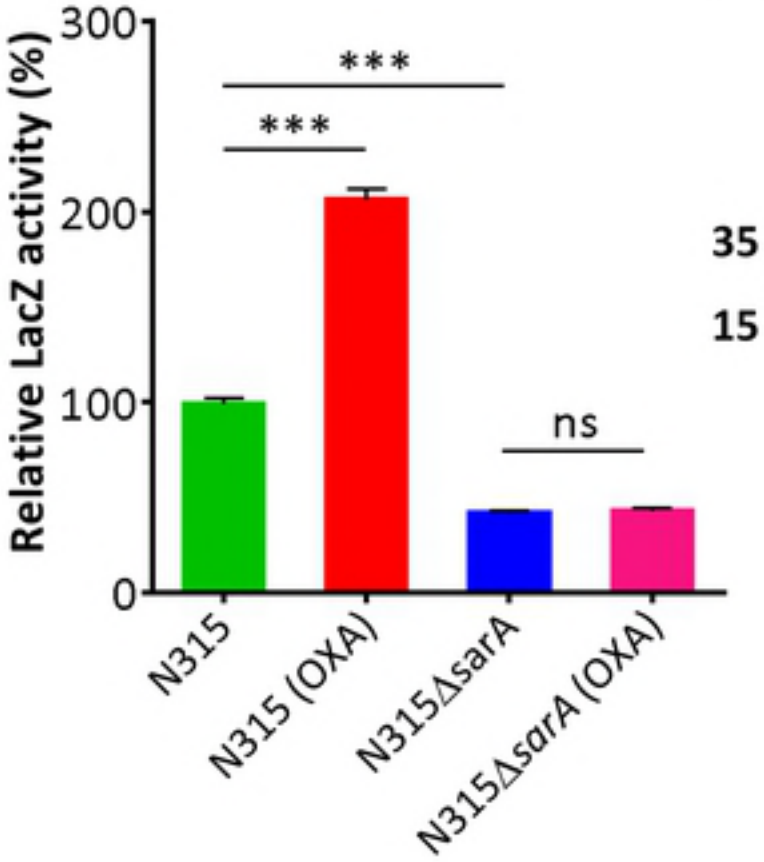

B

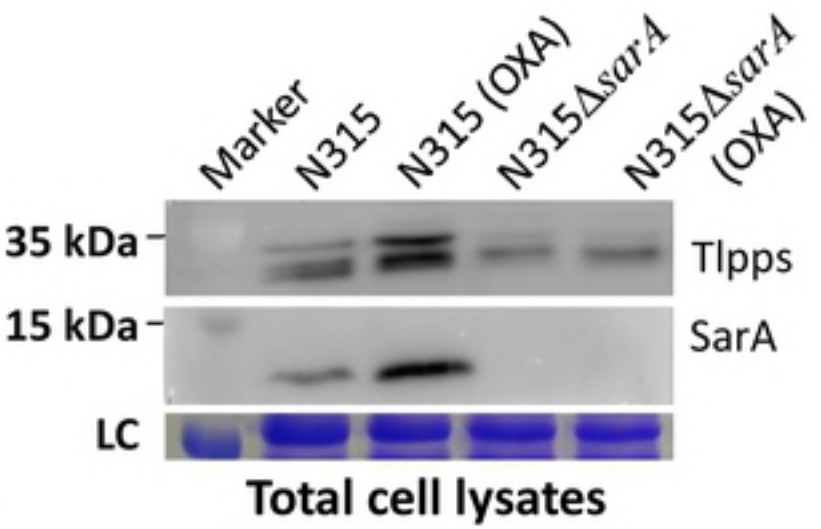

C

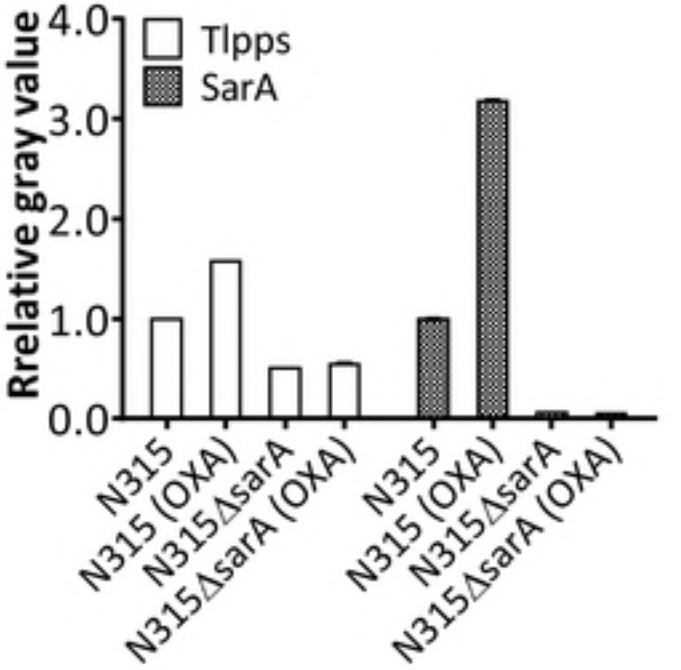

D

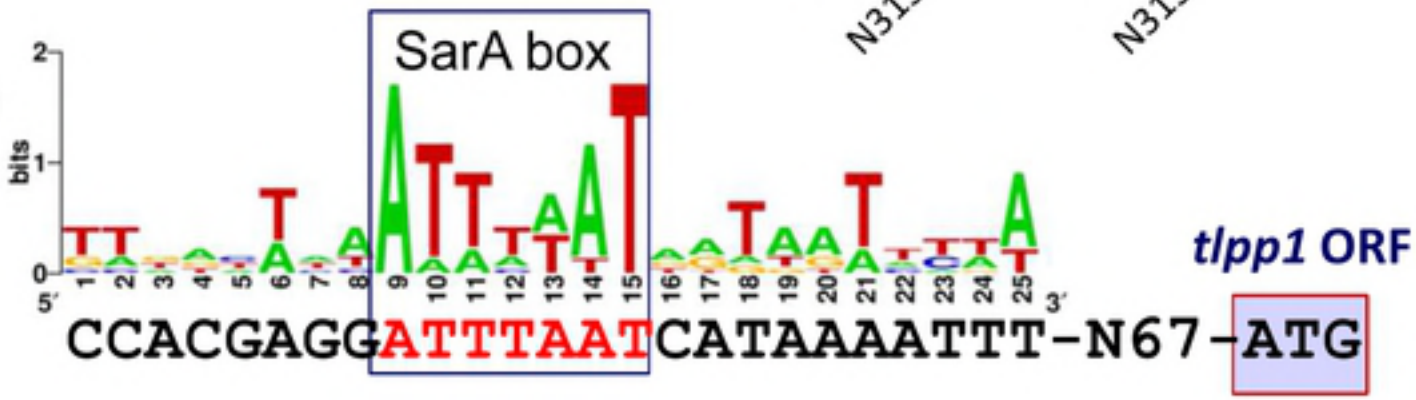

E

tlpps-P: CCACGAGGATTTAATCATAAAATTTCCTCTAGTATTATTAATATTGGAATTT-N40-ATG

tlpps-PM: CCACGAGGGGGGGGCATAAAATTTCCTCTAGTATTATTAATATTGGAATTT-N40-ATG

F

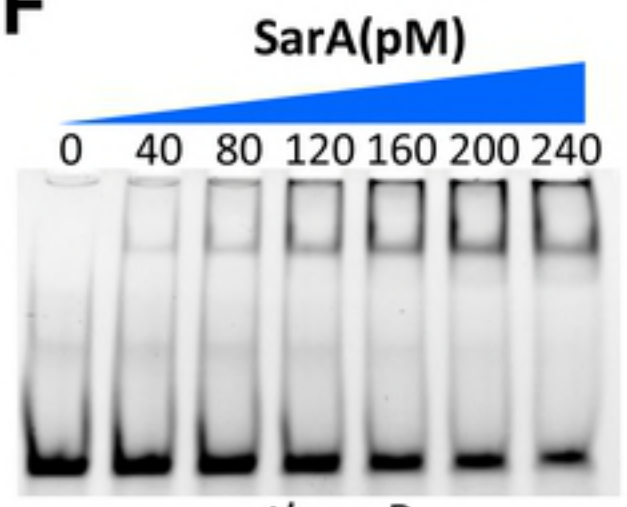

G

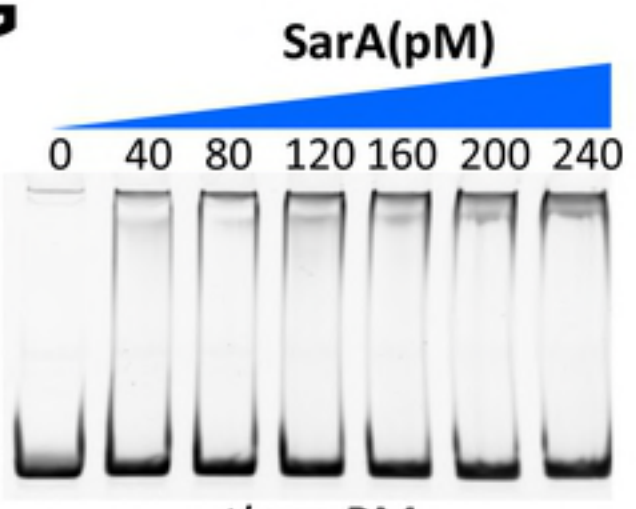

H

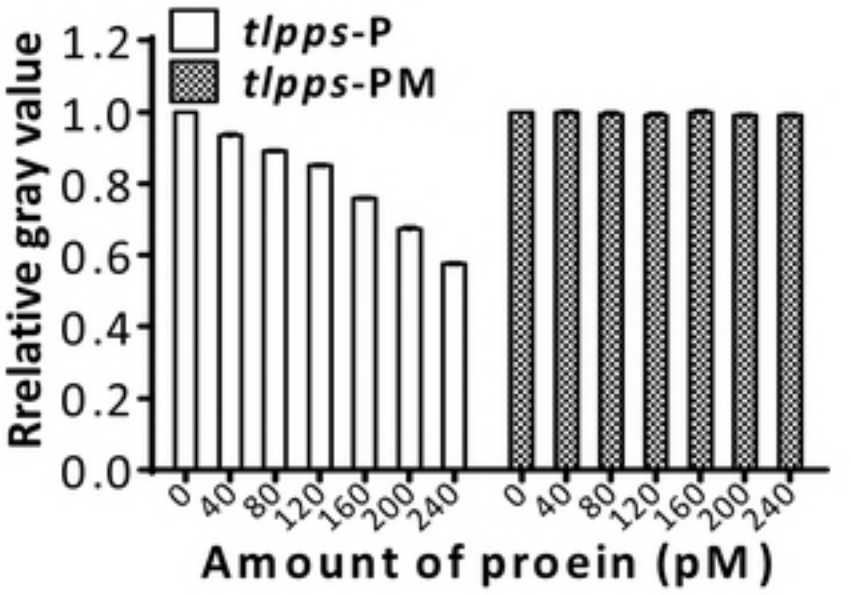

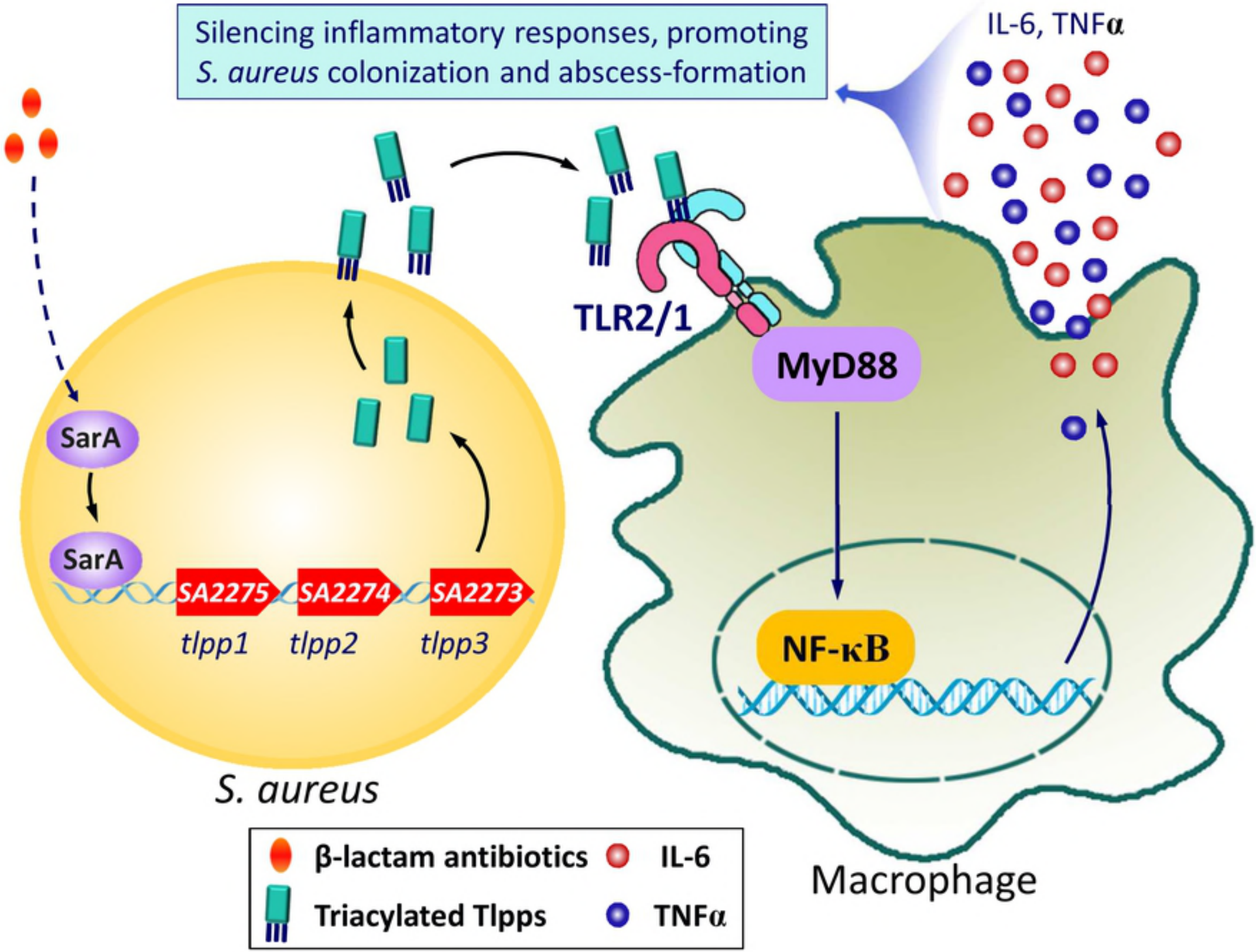
Silencing inflammatory responses, promoting
S. aureus colonization and abscess-formation
IL-6, TNFα
TLR2/1
MyD88
SarA
SarA
SA2275
SA2274
SA2273
tlpp1
tlpp2
tlpp3
NF-κB
S. aureus
Macrophage
β-lactam antibiotics
IL-6
Triacylated Tlpps
TNFα

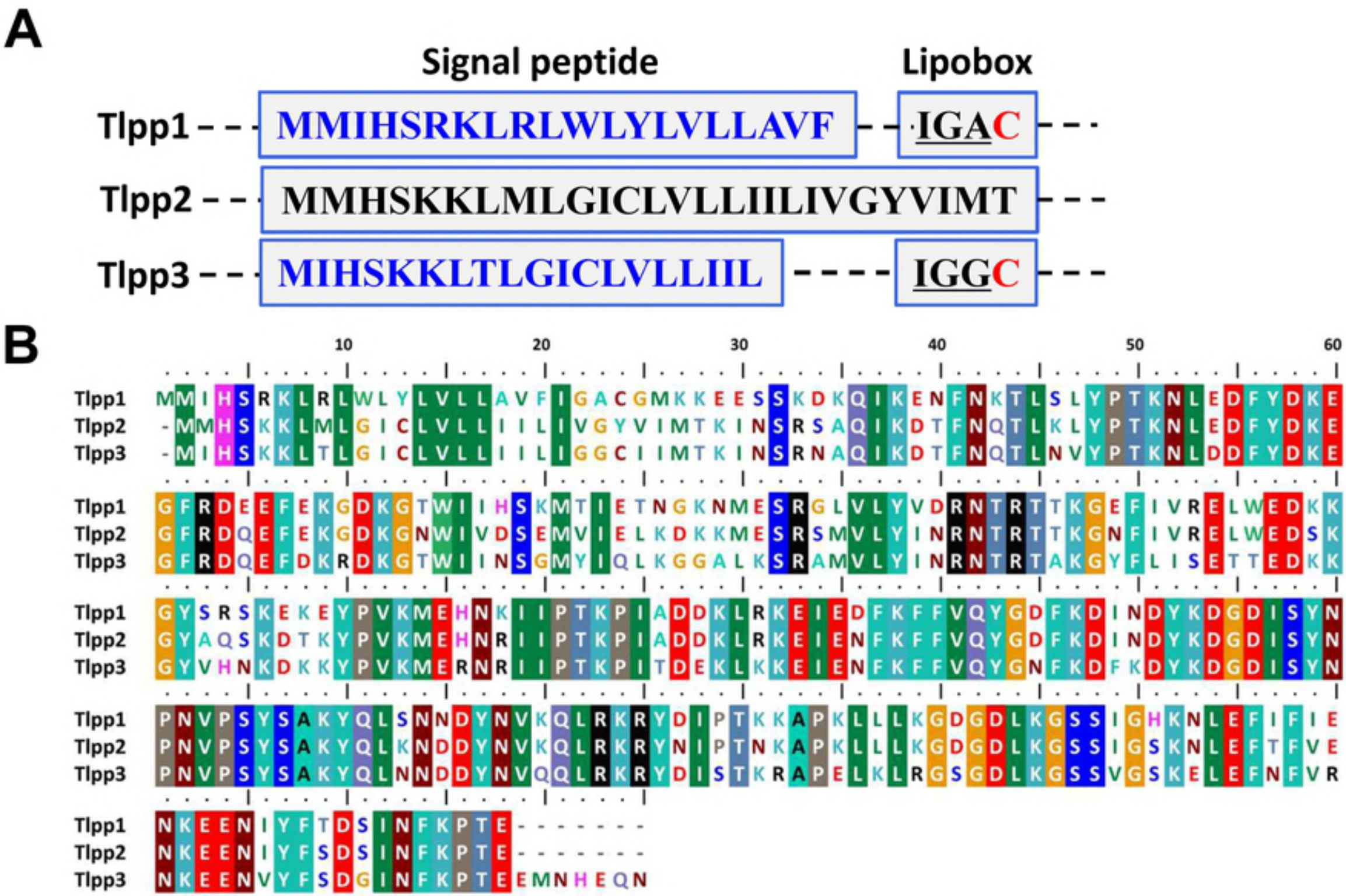
A
Signal peptide
Lipobox
Tlpp1
MMIHSRKLRLWLYLVLLAVF
IGAC
Tlpp2
MMHSKKLMLGICLVLLIILIVGYYVIMT
Tlpp3
MIHSKKLTLGICLVLLIIL
IGGC
B
10
20
30
40
50
60
Tlpp1
Tlpp2
Tlpp3

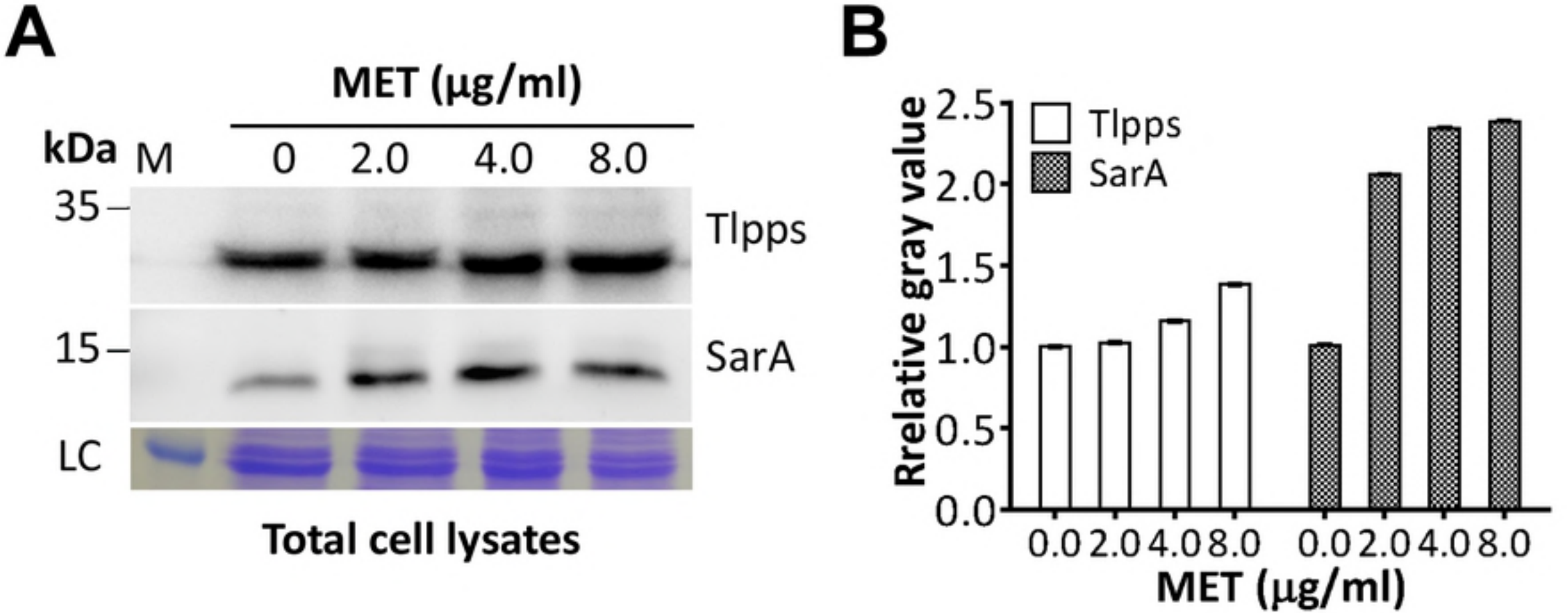
A
MET (μg/ml)
kDa
M
0
2.0
4.0
8.0
35
15
Tlpps
SarA
LC
Total cell lysates
B
Rrelative gray value
2.5
2.0
1.5
1.0
0.5
0.0
Tlpps
SarA
0.0 2.0 4.0 8.0 0.0 2.0 4.0 8.0
MET (μg/ml)

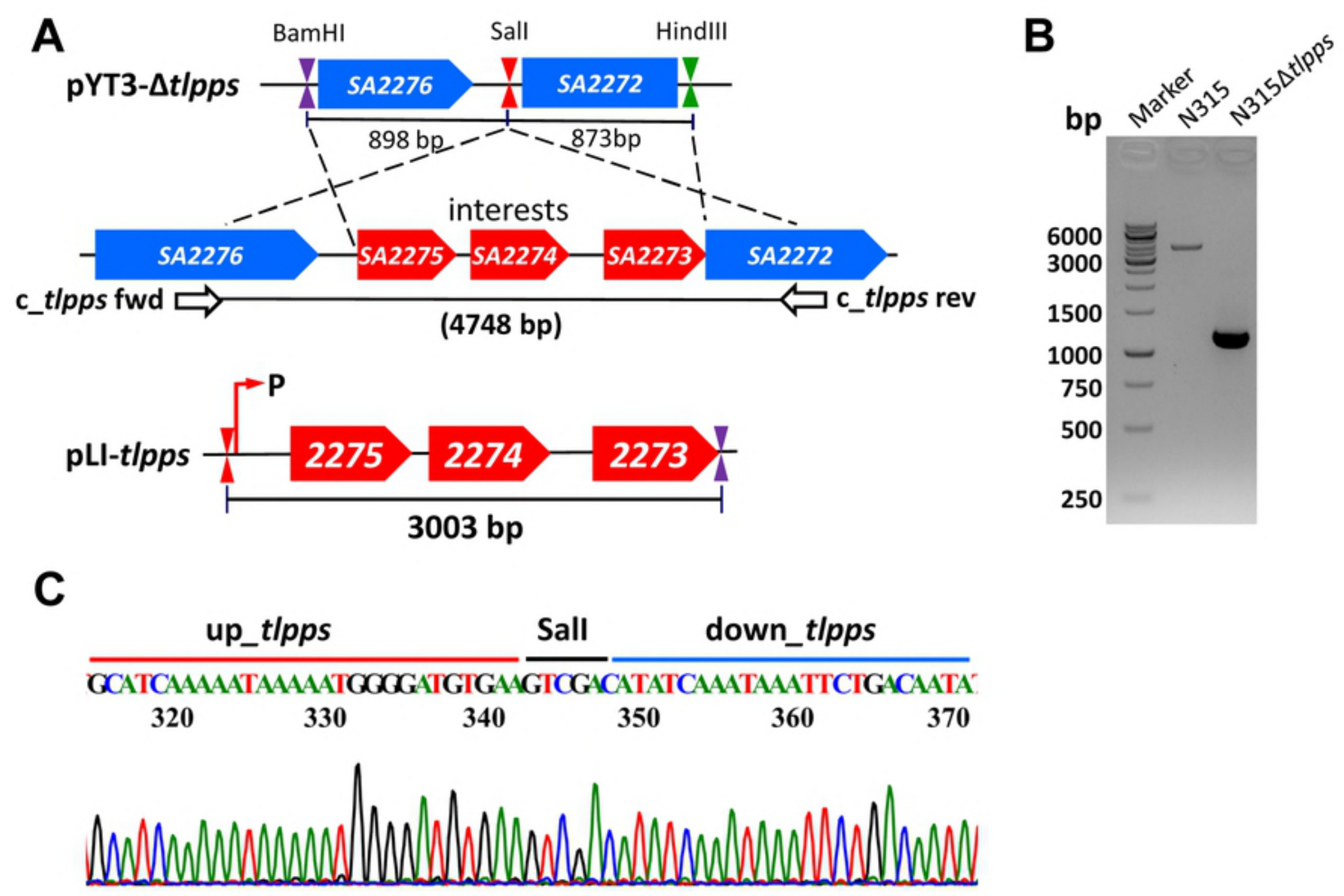
A
BamHI
SalI
HindIII
pYT3-Δtlpps
SA2276
SA2272
898 bp
873bp
interests
SA2276
SA2275
SA2274
SA2273
SA2272
c_tlpps fwd
c_tlpps rev
(4748 bp)
P
pLI-tlpps
2275
2274
2273
3003 bp
B
bp
Marker
N315
N315Δtlpps
6000
3000
1500
1000
750
500
250
C
up_tlpps
SalI
down_tlpps
GCATCAAAAATAAAAATGGGGATGTGAAGTCGACATATCAAATAAATTCTGACAATA
320
330
340
350
360
370

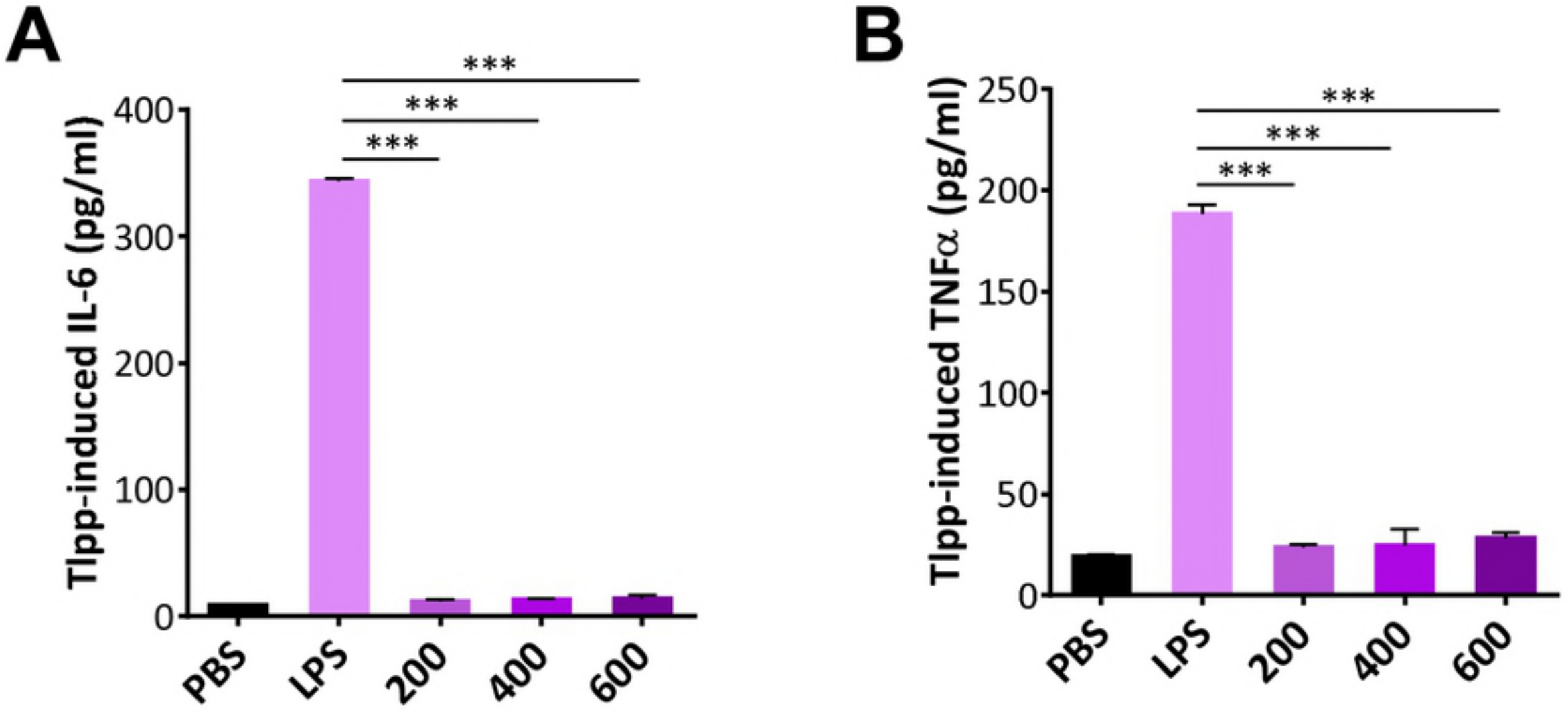
A
Tlpp-induced IL-6 (pg/ml)
400
300
200
100
0
***
***
***
PBS
LPS
200
400
600
B
Tlpp-induced TNFα (pg/ml)
250
200
150
100
50
0
***
***
***
PBS
LPS
200
400
600

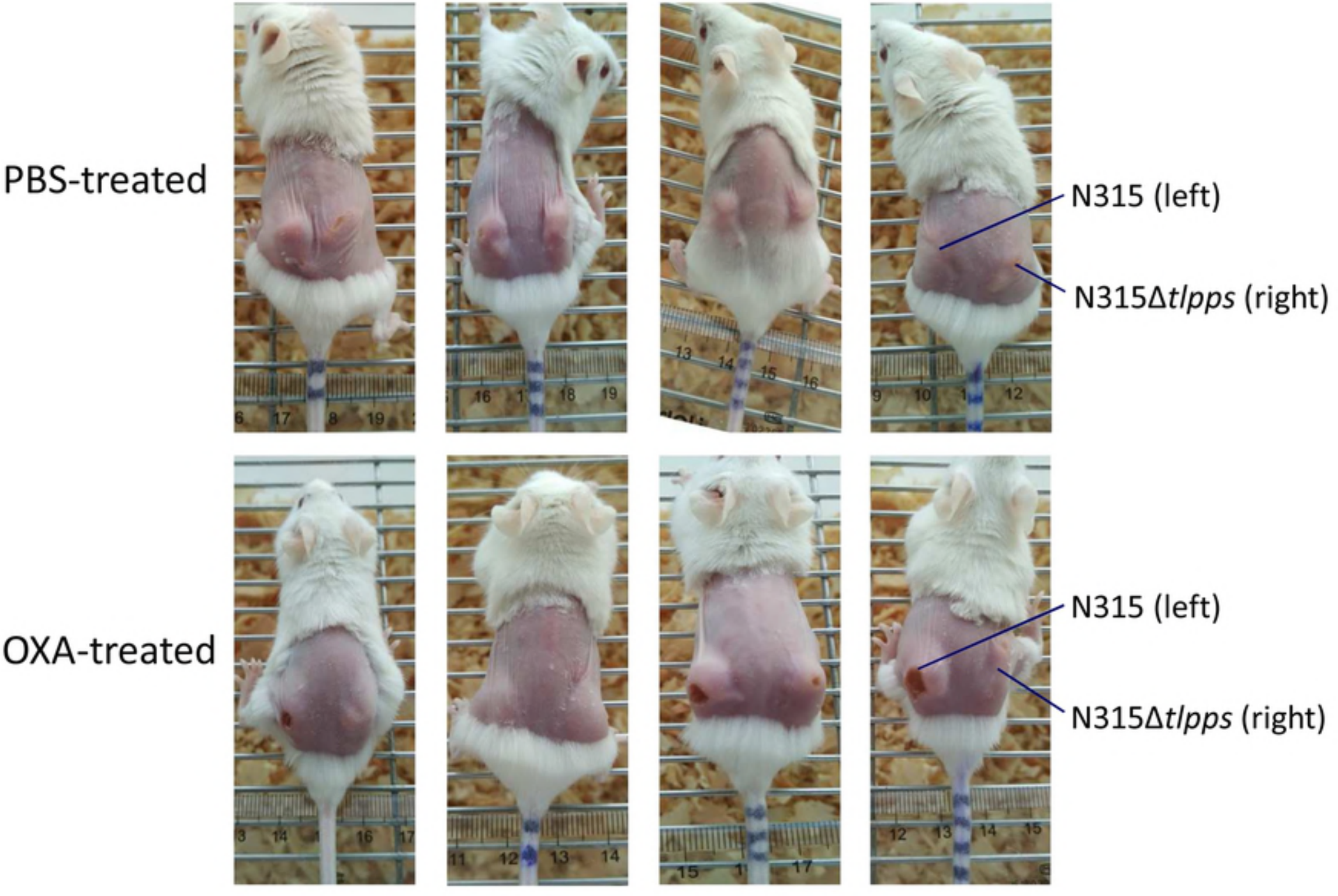
PBS-treated
N315 (left)
N315Δ*tlpps* (right)
OXA-treated
N315 (left)
N315Δ*tlpps* (right)

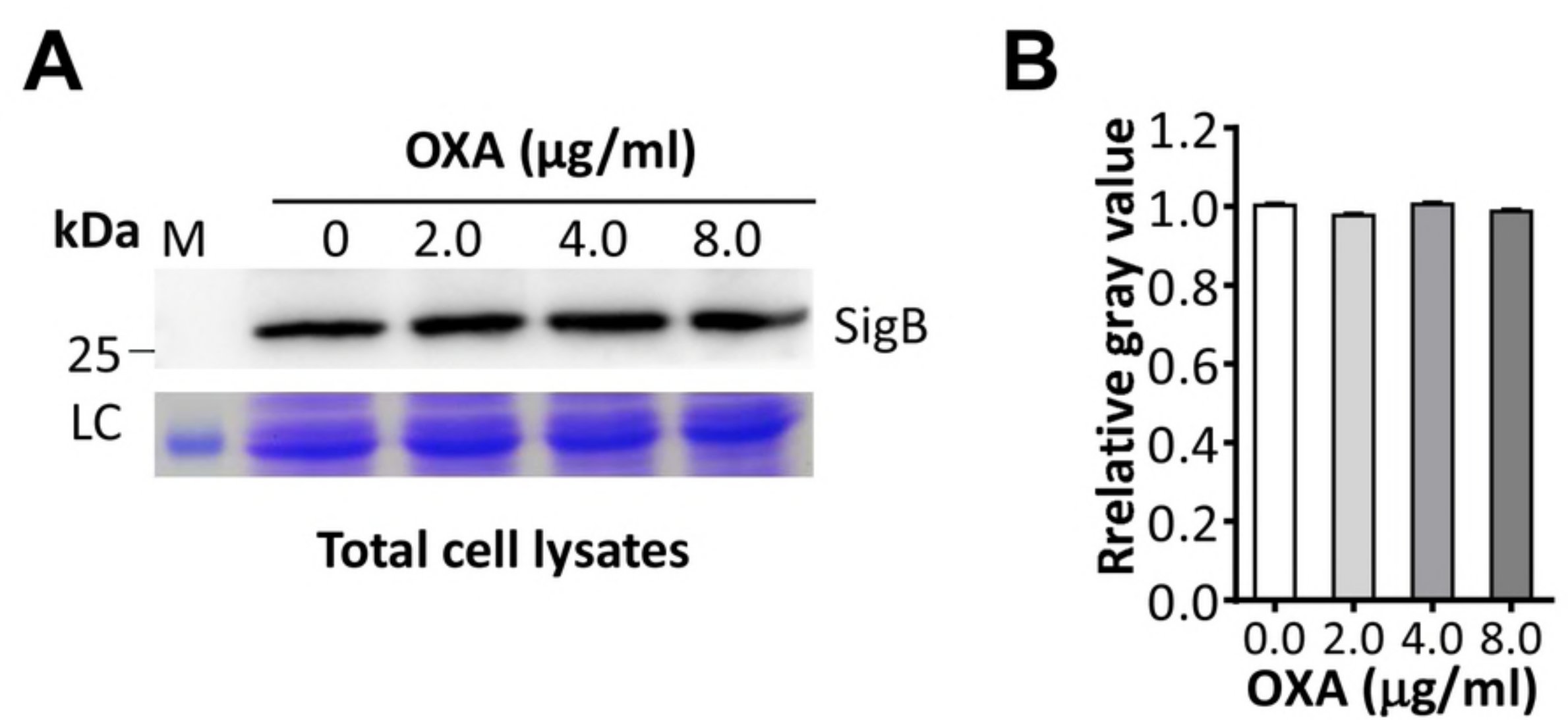
A
OXA (μg/ml)
kDa
M
0
2.0
4.0
8.0
25
SigB
LC
Total cell lysates
B
Rrelative gray value
1.2
1.0
0.8
0.6
0.4
0.2
0.0
0.0 2.0 4.0 8.0
OXA (μg/ml)

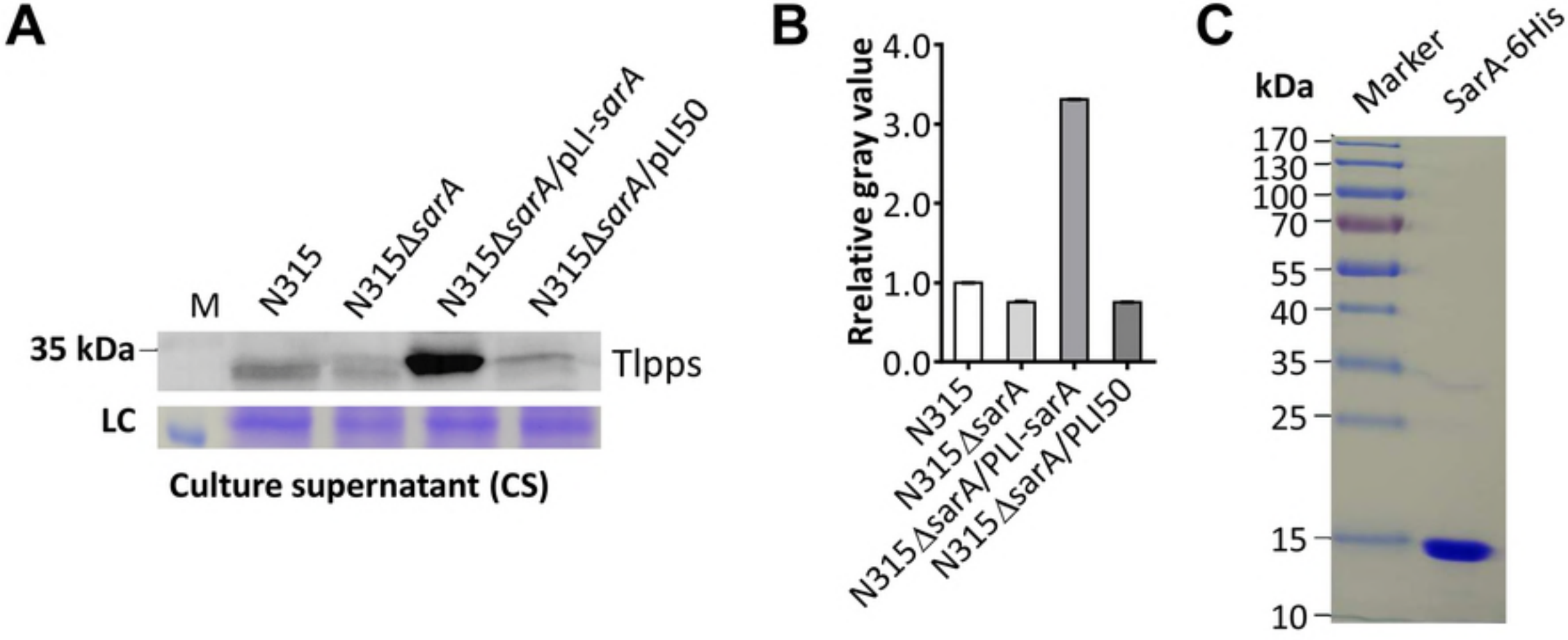
A
M
N315
N315ΔsarA
N315ΔsarA/pLI-sarA
N315ΔsarA/pLI50
35 kDa
Tlpps
LC
Culture supernatant (CS)
B
Rrelative gray value
4.0
3.0
2.0
1.0
0.0
N315
N315ΔsarA
N315ΔsarA/PLI-sarA
N315ΔsarA/PLI50
C
kDa
Marker
SarA-6His
170
130
100
70
55
40
35
25
15
10

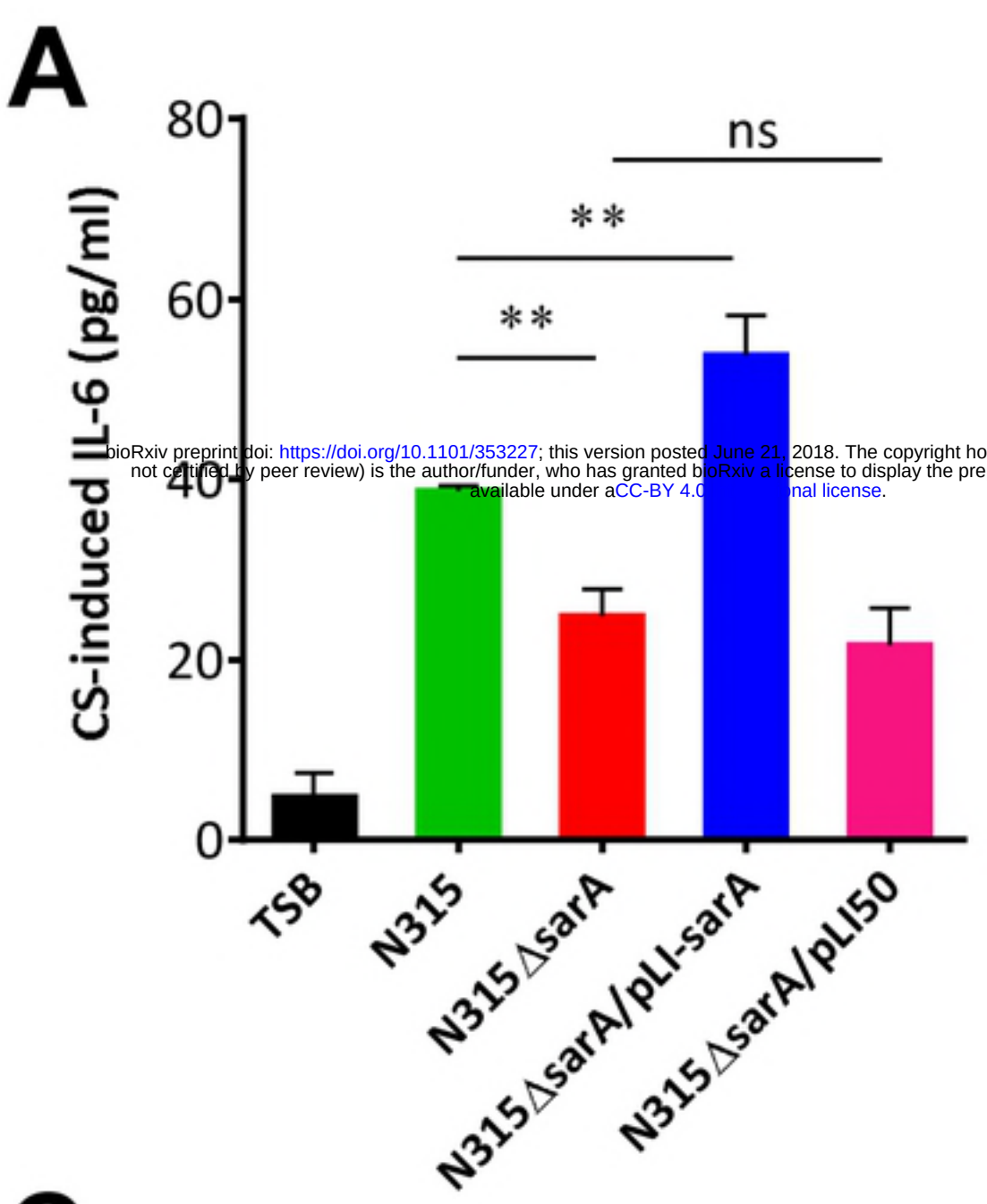

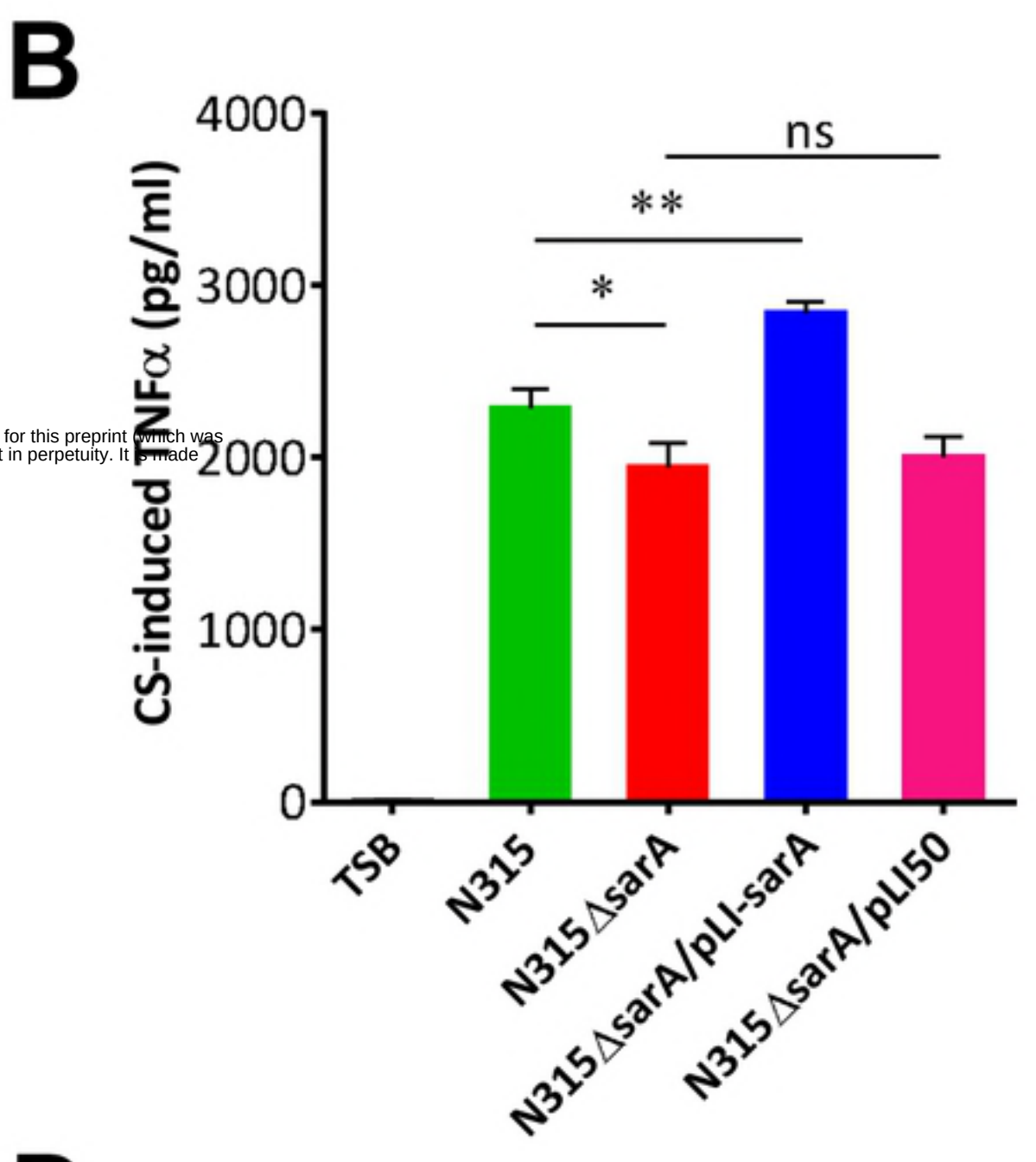

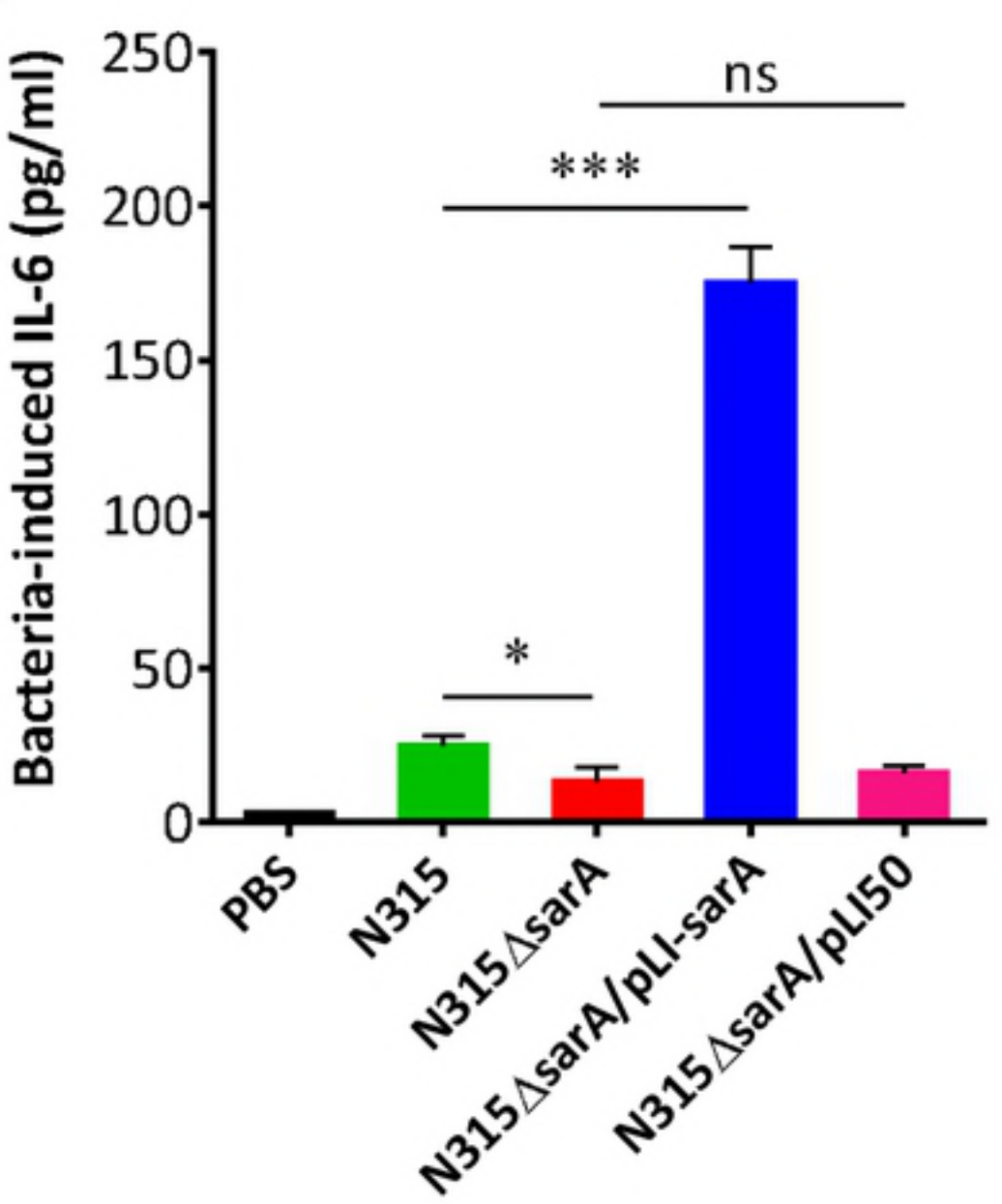

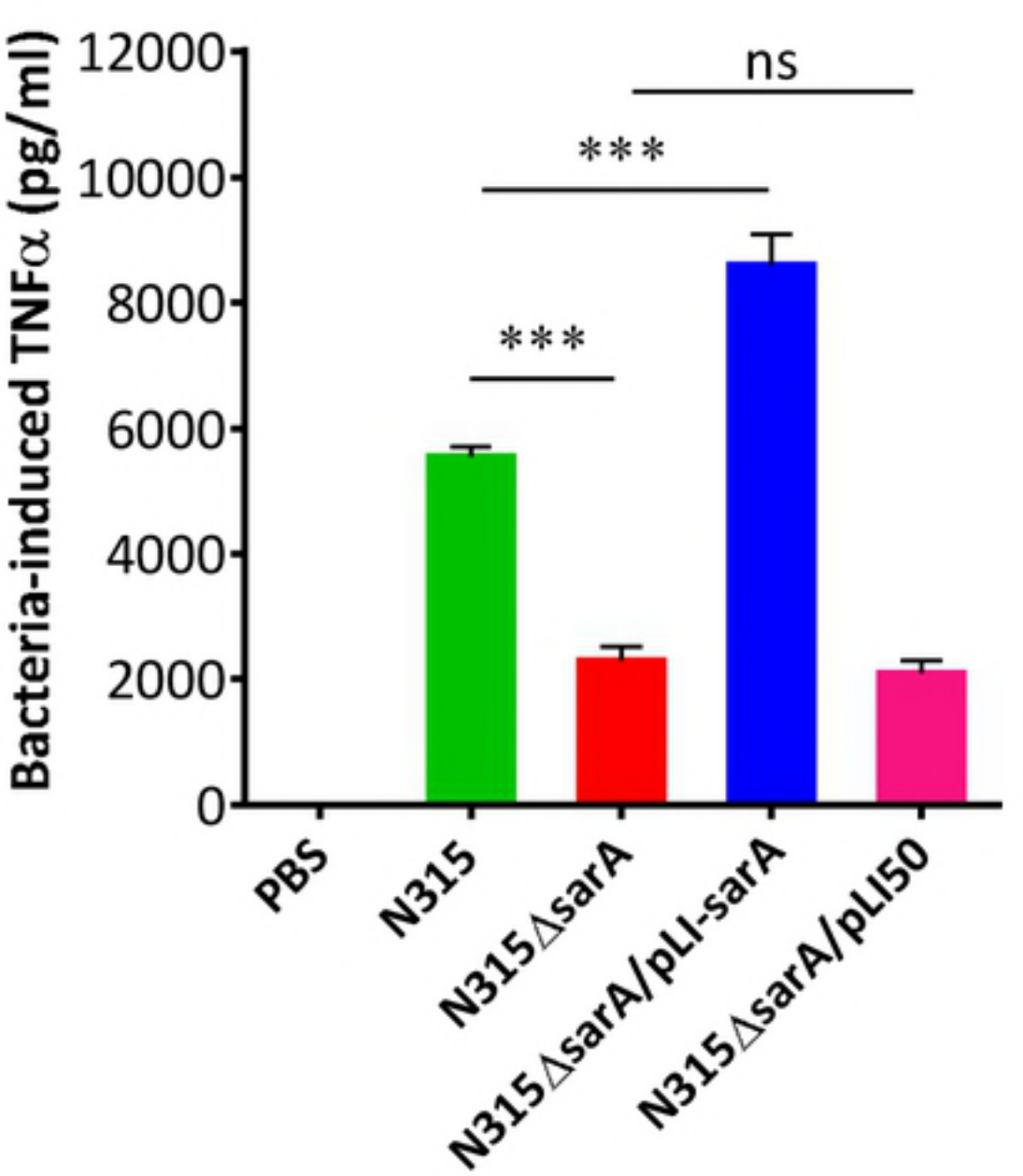

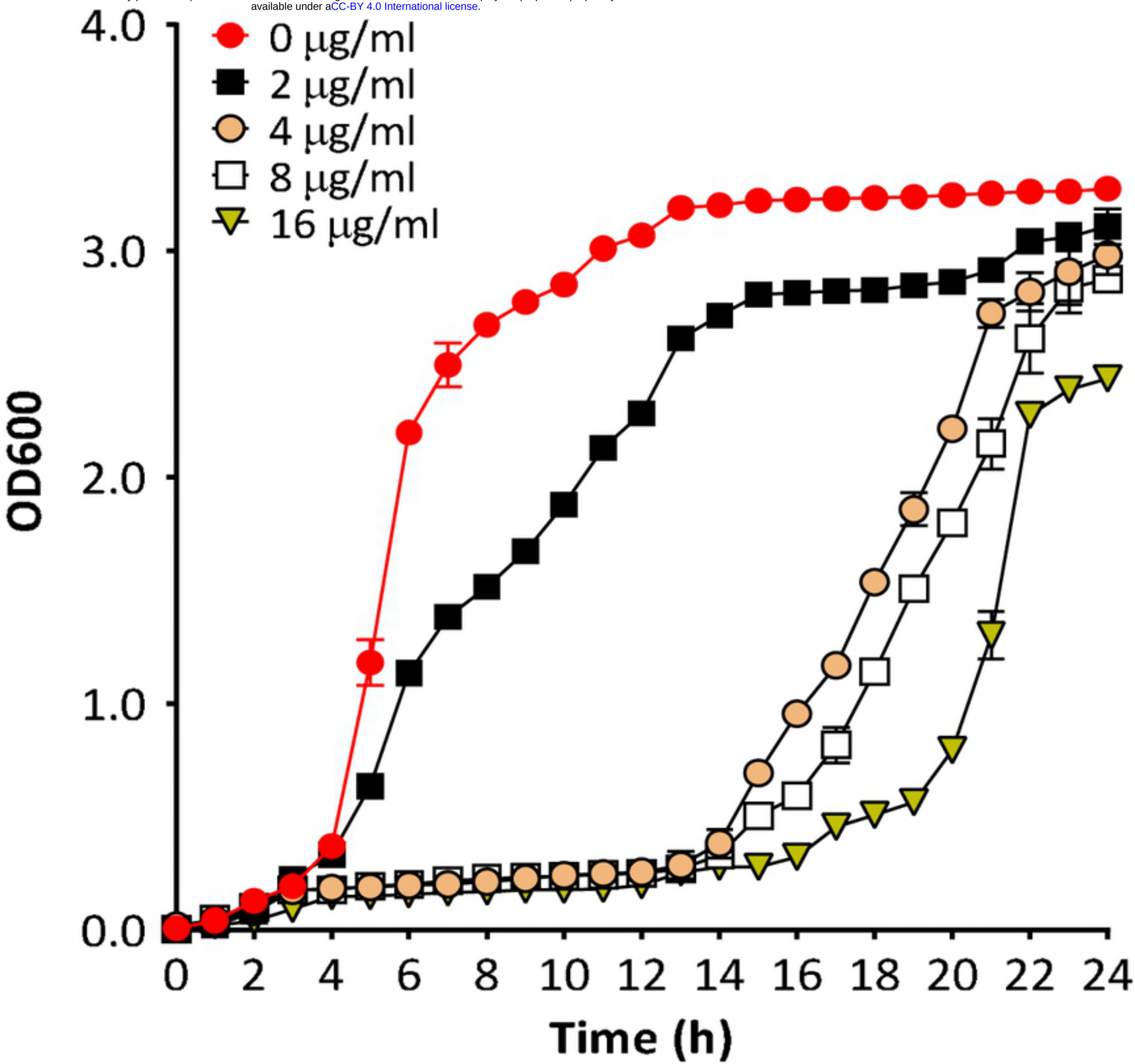

Fig. 1D

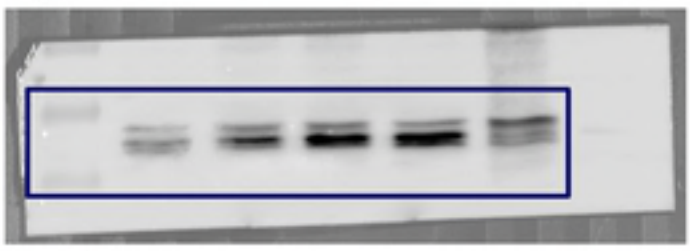

Fig. 2D

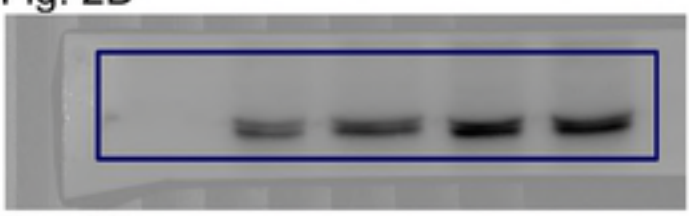

Fig. 2F

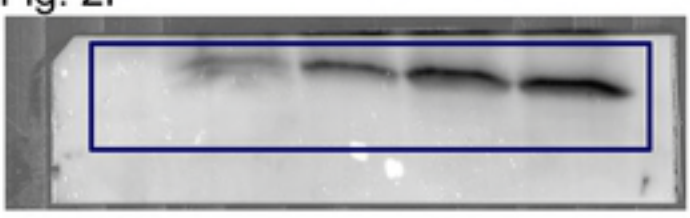

Fig. 3C

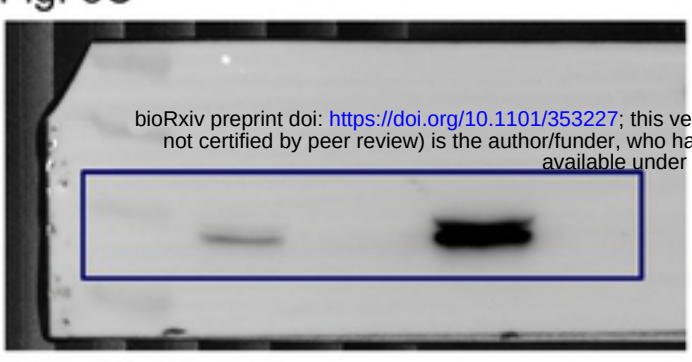

Fig. 2H

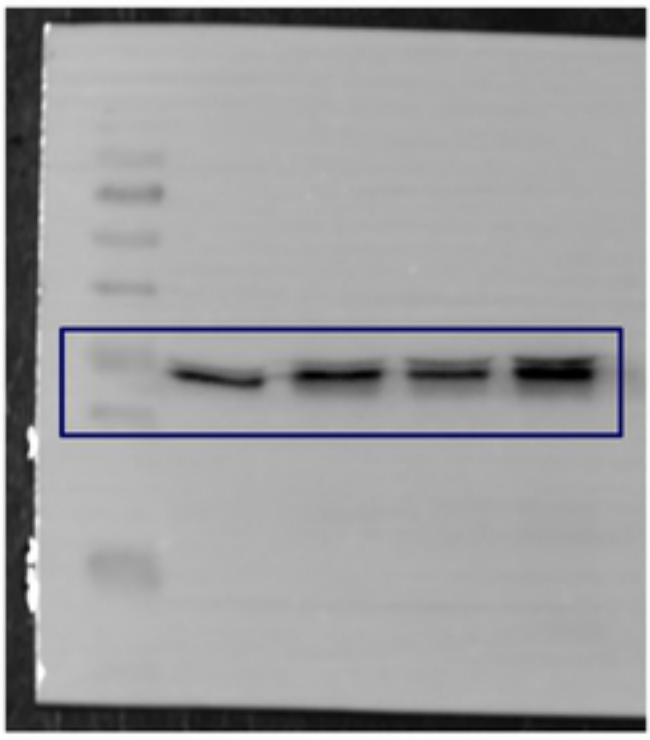

Fig. 3F

Fig. 6B (Tlpps)

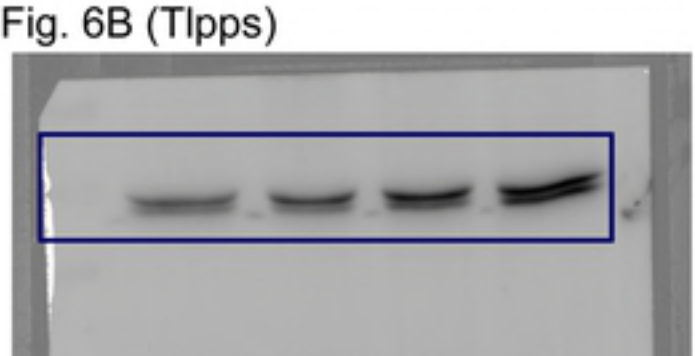

Fig. 6B (SarA)

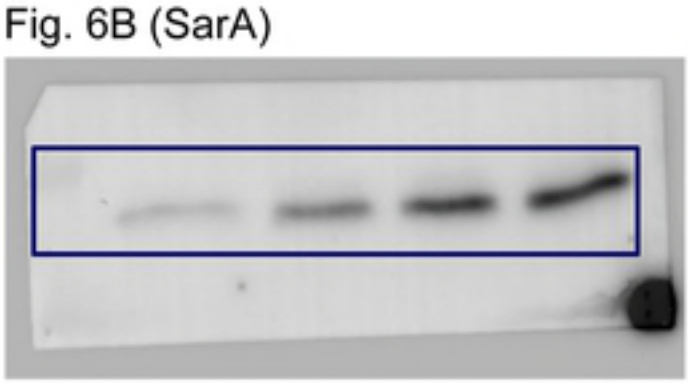

Fig. 6D (Tlpps)

Fig. 6D (SarA)

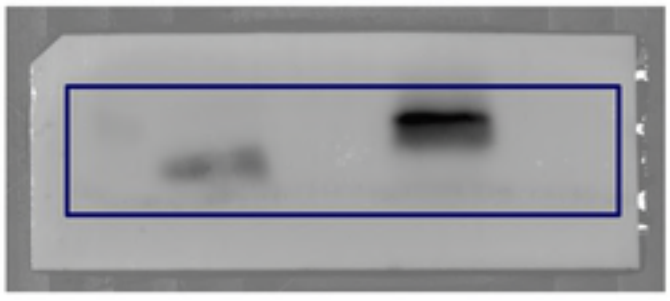

Fig. 7B (Tlpps)

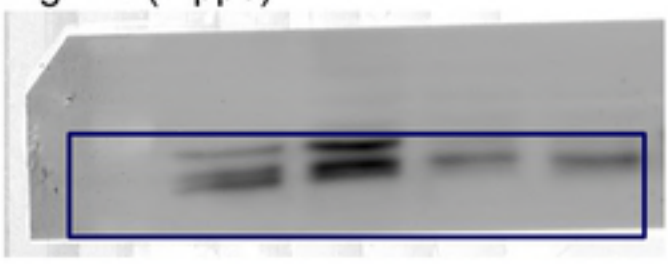

Fig. 7B (SarA)

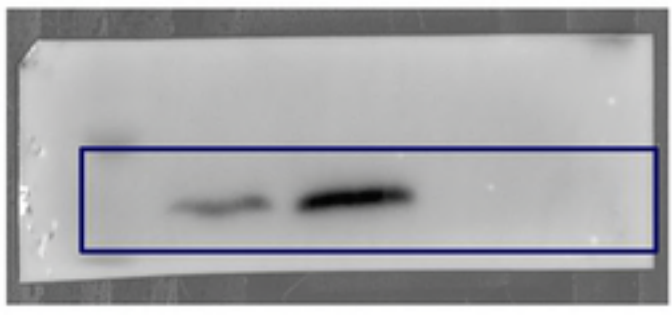

Supplementary Fig. 2A (Tlpps)

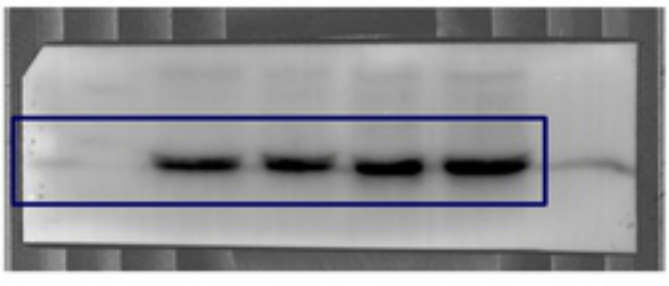

Supplementary Fig. 2A (SarA)

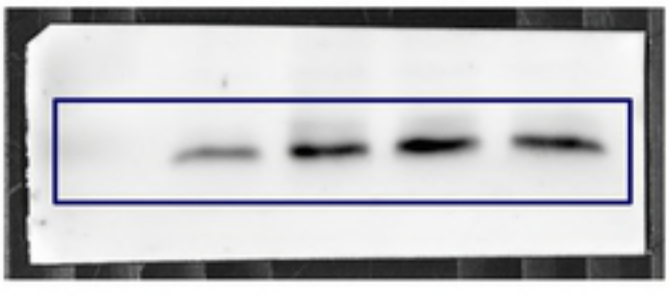

Supplementary Fig. 6A

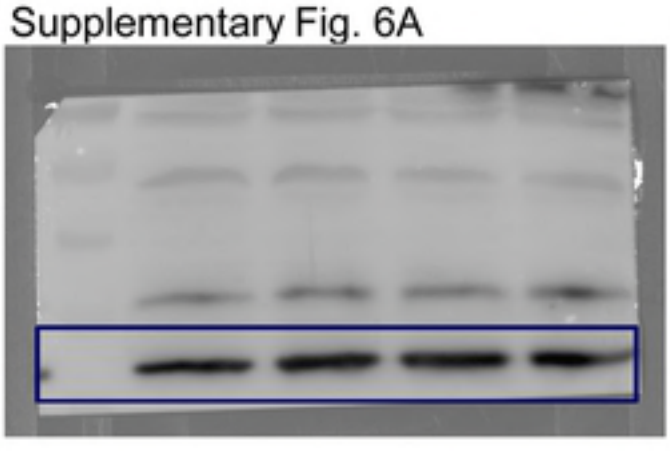

Supplementary Fig. 7A